The Holocene

HOLOCENE DUST IN EAST ANTARCTICA: PROVENANCE AND VARIABILITY IN TIME AND SPACE

Journal:	*The Holocene*
Manuscript ID	HOL-19-0005.R1
Manuscript Type:	Review
Date Submitted by the Author:	n/a
Complete List of Authors:	Delmonte , Barbara; Universita degli Studi di Milano-Bicocca Winton, Victoria; Curtin University; British Antarctic Survey Baroni, Mélanie; CNRS, IRD, INRA, Coll France, CEREGE Baccolo, Giovanni; Universita degli Studi di Milano-Bicocca Hansson, Margareta; Stockholms Universitet Andersson, Per; Naturhistoriska riksmuseet Baroni, Carlo; Universita degli Studi di Pisa Salvatore, Maria; Universita degli Studi di Pisa; CNR-Institute of Geosciences and Earth Resources Lanci, Luca; Department of Pure and Applied Science, University of Urbino "Carlo Bò", Maggi, Valter; Universita degli Studi di Milano-Bicocca
Keywords:	Ice Cores, Dust, Holocene, East Antarctica, Provenance, Dust stratigraphy
Abstract:	In this paper we provide a comprehensive overview of the state-of-knowledge of dust flux and variability in time and space in different sectors of East Antarctica during the Holocene. By integrating literature data with new evidences, we discuss the dust flux and grain size variability during the current interglacial and its provenance in the innermost part of the East Antarctic plateau as well as in peripheral regions located close to the Transantarctic Mountains. The local importance of aeolian mineral dust aerosol deflated from low-elevation areas of peripheral East Antarctica is also discussed in the light of new data from several coastal, low elevation sites.

Revised for the Special Issue on Holocene Dust Dynamics | 2019

HOLOCENE DUST IN EAST ANTARCTICA: PROVENANCE AND VARIABILITY IN TIME AND SPACE

Barbara Delmonte*[1], Holly Winton[2,3], Mélanie Baroni[4], Giovanni Baccolo[1], Margareta Hansson[5], Per Andersson[6], Carlo Baroni[7,8], Maria Cristina Salvatore[7,8], Luca Lanci[9] and Valter Maggi[1]

1 Department of Environmental and Earth Sciences, University of Milano-Bicocca, Milan, Italy

2 Physics and Astronomy, Curtin University, Perth, Western Australia, 6102, Australia

3 British Antarctic Survey ,High Cross, Madingley Road, Cambridge CB3 0ET, United Kingdom

4 Aix Marseille Univ, CNRS, IRD, INRA, Coll France, CEREGE, Aix-en-Provence, France

5 Department of Physical Geography, Stockholm University, S-106 91 Stockholm, Sweden

6 Swedish Museum of Natural History, Frescativägen 40, 104 05 Stockholm, Sweden

7 Department of Earth Sciences, University of Pisa, Via S. Maria n. 53, 56126, Pisa, Italy

8 CNR-Institute of Geosciences and Earth Resources, Via G. Moruzzi n.1, 56124, Pisa, Italy

9 Department of Pure and Applied Science, University of Urbino "Carlo Bò", Via S. Chiara 27, 61029 Urbino (PU), Italy

(*corresponding author: barbara.delmonte@unimib.it)

Abstract

In this paper we provide a comprehensive overview of the state-of-knowledge of dust flux and variability in time and space in different sectors of East Antarctica during the Holocene. By integrating literature data with new evidences, we discuss the dust flux and grain size variability during the current interglacial and its provenance in the innermost part of the East Antarctic plateau as well as in peripheral regions located close to the Transantarctic Mountains. The local importance of aeolian mineral dust aerosol deflated from low-elevation areas of peripheral East Antarctica is also discussed in the light of new data from several coastal, low elevation sites.

INTRODUCTION

Mineral dust deflated from continental landmasses of the Southern Hemisphere reaches high elevation sites of central East Antarctica after transport in the mid-to-high troposphere over very long distances greater than 1000 km (Lambert et al., 2008; Petit et al., 1999). After deposition onto the polar plateau, dust buried in snow and ice layers can be studied through deep ice core stratigraphies and can be used to document past atmospheric circulation variability.

During the late Quaternary, dust influx to the polar East Antarctic plateau was a factor ca. 25 higher during glacial periods than during interglacials, when the dust concentration in snow and ice layers reached extremely low levels, especially in the interior of the ice sheet (Petit et al., 1999; Lambert et al., 2008). Among the causes responsible for the drastic glacial/interglacial change of dust concentration in polar ice, a primary role is played by changed environmental conditions within dust source areas modulating the so-called source "intensity" (Delmonte et al., 2017). Dust atmospheric lifetime and snow accumulation rate in Antarctica, which are factors related to some degree to climate and the hydrological cycle (Petit & Delmonte, 2009, Markle et al., 2018), additionally played a key role. Dust in central East Antarctica is remotely sourced from extra-Antarctic continental landmasses, including South America and possibly other areas in the Southern Hemisphere (Basile et al., 1997; Delmonte et al., 2007, 2008, 2010a; Revel-Rolland et al., 2006; Gaiero, 2007; Gaiero et al., 2007; Gili et al., 2016, 2017; Revel-Rolland et al., 2006; De Deckker et al., 2010). Given the remoteness of the sources and the very long transport distance, the Holocene dust depositional flux in central East Antarctica is the lowest on Earth, and the grain size of background mineral aerosol is very small (<5 µm diameter). Even so, slight (0.3-0.6 µm) variations in the modal value of dust grain size mass distribution have been observed and associated to the varying strength of air subsidence over Antarctica and air inflow from low latitudes.

On the periphery of the East Antarctic plateau, close to the Transantarctic Mountains or to ice-free surfaces outcropping from the ice sheet as mountain peaks (nunataks), an important contribution to the input of fine dust particles into the local Antarctic atmosphere is provided by high-altitude exposed regoliths and glacial drifts, providing non-cohesive sediments immediately available for wind mobilization and transport. In Northern Victoria Land, for example, indication of a long history of wind erosion is provided by some high-elevation relict surfaces, sometimes displaying aeolian deflation pavements, exposed for millions of years (Baroni et al., 2004; Oberholzer et al., 2003, 2008; Di Nicola et al. 2012). During the Holocene, when the extremely low remote dust influx from extra-Antarctic sources is mixed in varying proportions with locally-sourced dust, the ice core dust record becomes sensitive to the regional climate and atmospheric circulation variability. This is the case for Talos Dome (Baccolo et al., 2018; Delmonte et al., 2010b, 2013; Albani et al., 2012) and Taylor Dome ice core records (Aarons et al., 2016), for example. The spatial dispersal of local sediments towards the interior of the ice sheet, however, is definitely negligible or null, as revealed by spatial studies on a number of firn cores from the pre-industrial period (Delmonte et al., 2013).

At low elevation, on the coastal fringes of the continent close to sea level, East Antarctic ice-free areas are more abundant although, on the whole, their extension represents only about 1% of Antarctica. The most extensive ice-free areas in East Antarctica are located in Northern and Southern Victoria Land and in the southern Transantarctic Mountains. Although discontinuously distributed, other ice-free areas much less extended than these exist in coastal Adélie Land, Wilkes Land, Prince Charles Mountains, Endreby Land and Dronning Maud Land (figure 1). In these regions, the local dust deposition at low elevation sites can be orders of magnitude greater than the pristine remote background measured in ice cores from the inner plateau (Atkins & Dunbar 2009, Chewings et al. 2014). In addition, in some settings Antarctic dust can become an important potential source of bio-available Fe to the ocean (Winton et al. 2014, 2016a, 2016b).

The intent of this paper is to provide a comprehensive overview of the state-of-knowledge of dust flux and of its variability in time and space in different sectors of East Antarctica during the Holocene. We divide this paper in three sections. First, we present an overview of the main issues coming from studies of dust influx and transport variability in central East Antarctica during the Holocene, preceded by a brief excursion of the most well-established methods for analyzing dust concentration and grain size in polar ice cores. In this first section, we also present some new, high-resolution results from a late Holocene section of the new SOLARICE ice core, central East Antarctica. Then, we discuss Holocene dust provenance both in the innermost part of the East Antarctic plateau, at different sites located along a transect following nearly similar latitude but different longitude, and in marginal sites of Victoria Land close to ice-free areas that are of unique importance in terms of regional paleo-climatic and paleo-environmental reconstructions. Finally, the third and last part of this paper is focused on the local importance of aeolian mineral dust aerosol deflated from dusty low-elevation areas of Antarctica such as McMurdo Sound, and new data from Dronning Maud Land and the Bunger Hills Oasis, in Queen Mary Coast, Wilkes Land. All throughout this paper, literature data are integrated with new evidences from this work; we recommend the reader to refer to the supplementary material for details about samples and methods, and for additional data.

DUST CONCENTRATION, FLUX AND GRAIN-SIZE IN CENTRAL EAST ANTARCTICA THROUGHOUT THE HOLOCENE

TECHNIQUES FOR DUST CONCENTRATION AND GRAIN-SIZE MEASUREMENTS

Since the early 1980's microparticle counting and sizing on discrete ice core meltwater samples has been typically performed through the Coulter Counter technique (Petit et al., 1981; Fujii and Ohata, 1982), which measures the short-term changes in the electrical impedance across a very small aperture (typically 30 or 50 µm) through which particles suspended in a very diluted electrolyte solution are forced to flow. Since this change is proportional to the particle volume, a particle volume-size distribution spectrum - represented in terms of equivalent spherical diameter - can be obtained. Under the assumption of spherical particle shape and constant density (2.5 g/cm^3), the number- and mass-size distributions can be also obtained. The high sensitivity, precision and accuracy of Coulter Counter measurements have made this technique a reference for dust counting and sizing in polar ice cores. Today it is possible to measure by Coulter Counter concentrations of a few ppb over a high-resolution size spectrum of 400 log-size channels (or more) on less than 5 mL of sample. Optical counters measuring particle scattering (e.g. Fujii et al., 2003; Kawamura et al., 2017), optical extinction cross section (e.g. Ruth et al., 2002, 2008) or both extinction coefficients and optical thickness (Potenza et al., 2006) have also found application in ice-core research. The systematic application of extinction (scattering plus absorption)-based optical devices (e.g. Klotz Abakus laser sensor) coupled to continuous flow systems for high-resolution analyses of ice cores, has produced the longest undisturbed record of mineral dust aerosol spanning the last 800.000 years (Lambert et al., 2008) from the EPICA Dome C (DC) ice core. However, while optical particle counters can be easily calibrated with Coulter Counter mass concentrations, the non-negligible size distribution differences between extinction-based optical sensors and the Coulter Counter measurements caused by the irregular shape of dust particles in ice core samples (Potenza et al., 2016), made it necessary to introduce a new calibration routine (Simonsen et al., 2018).

DUST FLUX VARIABILITY

Average Holocene and pre-industrial dust mass concentrations and fluxes are reported in table 1 for different ice and firn cores from the East Antarctic plateau, along with additional information such as the investigated time interval, the average accumulation rate (from AICC2012 timescale, Veres et al., 2013), the altitude of each site and references for dust data. Locations of ice core sites are shown in figure 1. For the same sites, in figure 2 we show average dust fluxes calculated respectively for the Early, Middle and Lower Holocene sections of the cores.

Holocene dust fluxes from high-altitude inner plateau ice cores are definitely very low compared to other parts of the polar ice sheet: at Dome B, one of the highest ice core drilling sites considered, Holocene dust fluxes display the lowest average Holocene levels (0.28 mg m^{-2} per year; this work and Delmonte 2013). Similar average values are found at Vostok, Dome C (0.36 and 0.39 mg m^{-2} per year respectively; Delmonte et al., 2005) and at Dome Fuji (0.54 mg m^{-2} per year; Fujii et al., 2003; Kawamura et al., 2017). All these sites are located above 3000 m a.s.l. at similar latitude but different longitude, and receive dust from remote sources through high-altitude transport (Delmonte et al., 2004, 2005). The similarity is also confirmed by the general trend of dust flux variability during the Holocene at these sites. For all of them the temporal evolution of dust deposition reveals a general, slight, but continuous decrease across the Holocene. It was observed since the very first measurements on the EPICA DC ice core (Delmonte et al., 2002) and tentatively attributed to the gradual reduction of the dust reservoir available for wind deflation by progressive development of deflation pavement, pedogenesis, and increased vegetation cover on continents. Compared to the other high altitude inner sites, Dome Fuji shows an apparent flux increase during the Middle and Late Holocene, the reason for which is under investigation but could be an artifact of the lower resolution record (Kawamura et al., 2017).

When comparing inner plateau sites with peripheral sites such as Talos Dome and Taylor Dome, located close to the Transantarctic Mountains where important ice-free areas (nunataks, cliffs, ice free valleys, glacial moraines, etc) are located, some important differences arise. Compared to

Dome C, the average Holocene flux of fine particles (<5 µm) is ~4-5 times at Talos Dome and ~3 times at Taylor Dome. These differences are related to the local contribution from proximal ice-free areas within Victoria Land, which provide an additional regional dust input to the margin of the Antarctic plateau, as discussed below. Given these peculiarities, the stratigraphic records of mineral dust aerosol at Talos Dome and Taylor Dome (Albani et al., 2012; Baccolo et al., 2018; Aarons et al., 2016) is of exceptional importance to regional climate studies. Their analysis and interpretation made it possible to link the evolution of the local dust cycle with important climatic and environmental processes that are expressed in this Antarctic region. This is the case for the retreat of the Ross Sea ice shelf and the opening of the Ross Sea embayment occurred after the deglaciation and during the Early Holocene. In that period the drastic reduction of dust influx from remote glacial sources allowed local dust dynamics to emerge and become recognizable in ice core records.

In the South Atlantic sector of the Plateau, the dust flux at EPICA DML is also remarkably higher than in central plateau sites, a factor ~3-4 compared to Dome C (figure 2). The higher flux is related to the proximity of EPICA DML site to Southern South America, that is believed to be the major dust source at the site (see below), and possibly to the further contribution from additional sources (Wegner et al. 2015).

GRAIN-SIZE VARIABILITY CONTROLLED BY SECULAR-SCALE OSCILLATIONS

Holocene dust minerals deposited at Dome C (Gaudichet et al., 1986) typically consist of feldspars (k-feldspars and plagioclase), quartz and its polymorphs, phyllosilicates (e.g. micas such as muscovite, illite and other clay minerals), Fe, Al and Ti oxides in variable amounts. These particles display variable shape (Potenza et al., 2016) but systematically small grain size, as a consequence of the long and complex transport history, which occurred at high altitude prior to reaching the polar plateau (figure 3C). The maximum spherical equivalent of dust particles representing the typical background at Dome C is about 5 µm, while the volume-size distribution typically shows a lognormal distribution with a mode around 2 µm and a geometric standard deviation (σ_g) of ~1.8 (Delmonte et al., 2002). An exception is given by the presence of occasional tephra particles. They are related to explosive volcanic eruptions and their size can lead to significant deviations from the background values: in ice core samples it is not uncommon to observe volcanic particles with a diameter larger than 50 µm (Narcisi et al., 2005).

The background dust deposited in central East Antarctica displays only limited grain-size variations in time. In low-accumulation sites of central East Antarctica, where the effect of wet deposition (Unnerstad and Hansson, 2001) is negligible and deposition is essentially dry (Legrand and Mayewski, 1997), very small grain-size variations can be attributed to different atmospheric transport mechanisms. Relatively coarse dust (displaying abundance of coarse particles in the 3-5 µm diameter range) is related to dust-carrying air masses subjected to short and relatively low-altitude trajectories in the mid-troposphere. On the contrary, relatively fine dust (displaying abundance of fine particles in the 1-2 µm diameter range) is related to longer circumpolar atmospheric pathways, implying mass convergence in the middle troposphere and subsidence over the Antarctic Plateau (Krinner & Genthon, 2003). This possible explanation of dust grain size variability, proposed in some literature studies (Delmonte et al., 2005, 2017) can be applied both to Holocene and to glacial climate conditions. Actually, the dust transport time from the continental sources of the Southern Hemisphere to Antarctica, is definitely very long; according to a semi-empirical model (Petit & Delmonte, 2009), the mean dust transit time is about one month. This value is similar to the ones calculated using ^{222}Rn air concentration: they span from 22 to 28 days (Maenhaut et al., 1979; Genthon & Armengaud, 1995; Jacob et al., 1997; Li et al., 2008).

The EPICA DC ice core reveals clear oscillations of the grain-size parameters (Coarse Particle Percentage, CPP; i.e., the percentage of dust mass represented by particles within 3-5 µm spherical diameter) throughout the Holocene (Figure 3A), similarly to Vostok (Delmonte et al., 2005). This feature suggests that transport patterns at a given site may vary in time. Spectral analyses of the low resolution (discontinuous, one sample every ~50 years) Holocene grain-size stratigraphic profile of the Dome C and Vostok ice core, revealed that the energy is mostly spread between secular-scale bands of periodicity from 330-380 years to about 120 years. Interestingly, both EPICA DC and Vostok share a common significant frequency band around 200 years (Delmonte et al., 2005).

To better understand these periodic patterns, we present here the grain-size record from a new ice core drilled in Dome C in the framework of the SOLARICE research project (figure 3B). For the first time, dust size is measured continuously along the core on discrete samples of about 4-5 cm each (see supplementary material), representing about 2 years of accumulation at 100-200 m depth. According to a very preliminary timescale established by transferring SOLARICE to

AICC2012 chronology (Veres et al., 2013), the time period investigated here spans from about 3300 to 4500 years BP (in terms of depth from 125 to 160 m). The preliminary profile of CPP (figure 3B) confirms the presence of secular-scale oscillations (for example around ~360 years according to these preliminary data), similar to the ones already observed in low-resolution measurements. In addition, thanks to the higher temporal resolution, some high-frequency modes of variability arise. One of them is located around the ~80-90 years band, according to these preliminary data. These new results confirm the variable strength and localization of tropospheric air subsidence over Antarctica, which is related to local (< ~10^4-10^5 km^2) and regional (~10^6 -10^7 km^2) atmospheric dynamics, and highlight the importance of high-resolution ice core analyses for depicting high frequency modes of variability still hidden to discontinuous dust measurements. Studies on the SOLARICE ice core are going on in order to cover the entire Holocene; dust grain size variations will be compared, along with other climate and atmospheric proxies, to the cosmogenic-produced ^{10}Be isotope, in order to investigate possible links between solar activity and climate.

DUST PROVENANCES

CENTRAL EAST ANTARCTICA

Dust-provenance studies have been extensively carried out over the last decades in central East Antarctic ice cores. These studies were primarily focused on glacial periods because of the relatively high abundance of aeolian particles in the samples. Important changes in dust composition with respect to glacial periods arise during Holocene, although undoubtedly analytical errors associated to geochemical measurements become higher with respect to glacial age, as a consequence of the extremely low dust content, i.e. a few ng of dust per mL of sample.

Methods classically used include radiogenic isotope fingerprinting (Sr, Nd, Pb; Grousset et al., 1992; Basile et al, 1997; Delmonte et al., 2004, 2007; 2010a; Vallelonga et al., 2010), dust geochemical composition in terms of major, trace and Rare Earth Elements (Marino et al., 2008; Baccolo et al., 2018; Siggaard-Andersen et al., 2007; Gabrielli et al., 2010; Wegner et al., 2012), as well as mineralogical composition (Gaudichet et al., 1986, 1988) and dust ferromagnetic properties (e.g. Lanci et al., 2008).

For the glacial periods of the late Quaternary, these methods (figure 4) converge towards a dominant provenance from Patagonia/Tierra del Fuego (Grousset et al., 1992; Basile et al., 1997; Delmonte et al., 2004) including the Argentinean continental shelf at least during the sea-level low stand of MIS2 (Delmonte et al., 2017), with additional inputs from lower-latitude areas in South America (Gaiero et al., 2007; Gili et al., 2016, 2017) such as the Pampean region in the southern part of central western Argentina.

When compared to the last glacial period, MIS 2, Holocene dust in central East Antarctic ice cores is enriched in Ti, Al and K (Marino et al., 2008), more variable in time in terms of Rare Earth Elements (REE) patterns (Gabrielli et al., 2010; Wegner et al., 2012), characterized by a higher Lithium solubility (Siggaard-Andersen et al., 2007), relatively low-radiogenic in terms of $^{143}Nd/^{144}Nd$ (figure 4; Delmonte et al., 2007), and more highly-magnetic (Lanci et al., 2008) . In this respect, Pb isotope data are less indicative because the Pb input related to local (Antarctic) volcanoes veils the faint portion of Pb that is dust-related (Vallelonga et al., 2010).

All dust proxies cited above, agree on the variable dust composition during Holocene and likely during the last 15 ka, in opposition to the very uniform composition of dust during MIS2, and point towards a great mixture from multiple sources, an hypothesis that is also coherent with a possible contribution from different sub-sources inside the same continent.

The Holocene Sr-Nd radiogenic isotope composition of dust from Vostok and Dome C, compared with the vast literature data from potential source areas of the Southern Hemisphere available today, can be justified in different ways. A first possibility (Delmonte et al., 2007) implies a South American provenance only, from a weakened Patagonian source where periglacial dust production is drastically reduced, plus other low-latitude sources inside South America itself. These include loess from latitudes North of about 30°S, displaying isotopic characteristics very different from Patagonia/Southern Pampas aeolian sediments (Smith et al., 2003; Gaiero et al., 2004, 2007; Gili et al., 2017). Actually, while the similarity between loess samples from the southern Pampas and volcanic rocks of the southern Andes and Patagonia corroborates the possible Patagonian/southern Andean source for this loess (e.g. Smith et al., 2003), the isotopic fingerprint of loessic deposits further north becomes progressively distinct with respect to Patagonian/southern Andean basalts, and a possible role played by a source in the Puna Altiplano and/or the Bolivian Andes is also possible for these deposits (Iriondo et al., 1997), although debated (Sayago et al., 2001). An additional hypothesis to explain the isotopic signature of Holocene dust in central East Antarctica, is a direct transport from high-altitude Andean sources (such as the Altiplano-Puna plateau) to Antarctica via the jet stream (Gaiero et al., 2007; Delmonte et al., 2008; Siggaard-Andersen et al., 2007; Gili et al., 2016; 2017).

Other plausible scenarios for Holocene dust provenance in central East Antarctica imply a dominant contribution from South America plus a secondary Eastern Australian source (Revel-Rolland et al., 2006; De Deckker et al., 2010; Du et al., 2018) possibly integrated with a New Zealand source (Wegner et al., 2012; Neff and Bertler, 2015).

Almost certainly, the variable relative contribution from different sources in the course of the Holocene and the lack of one dominant dust source area account for the variable geochemical characteristics of Holocene dust in time. This marked temporal variability can be observed in different proxies, including dust magnetization (Lanci et al., 2008) which shows a very large variability with sometimes extremely high values that are unusual in crustal rocks. This suggests concentration of ferromagnetic minerals in association with Holocene and in general interglacial dust; one possible explanation relates high magnetization to an underestimated flux of micrometeorites (Lanci et al., 2012) in the size range of aeolian dust, which to date is still largely unconstrained (Duprat et al., 2007).

THE VICTORIA LAND MARGIN OF THE ICE SHEET

During glacial times the remote dust influx from South America influenced both the interior and the margin of the Antarctic ice sheet, overlooking any regional signal; after the massive deglacial dust decline and during Holocene, the margin of the East Antarctic plateau experienced a progressive regionalization of the dust cycle. This is clearly expressed by the Talos Dome (Baccolo et al., 2018; Delmonte et al., 2010, 2013; Albani et al., 2012) and Taylor Dome (Aarons et al., 2016) ice core dust records. These two ice cores offer a unique opportunity to study the regional history of marginal East Antarctica.

At Talos Dome in Northern Victoria Land, Holocene dust is not well-sorted, and is characterized by the occurrence of sporadic fine-silt grains of obvious local provenance. The isotopic (Figure 5, Delmonte et al., 2013) and elemental composition (Baccolo et al. 2018) of Holocene dust at Talos Dome is distinctly different from Dome C and Vostok (figure 5) and shows close similarity with local rock outcrops, mainly with regoliths developed on Ferrar dolerites. The importance of the doleritic outcrops as high altitude (2500–3000 m a.s.l.) dust sources in Northern Victoria Land was recently explained in relation with the geomorphology of the outcrops. Doleritic reliefs usually culminate with tabular ice-free plateaus (Mesa), consisting of high-altitude relict flat structural surfaces that given their altitude, are not affected by glacial/interglacial changes of ice sheet height (Baroni et al., 2004). Such elevated surfaces are intensively weathered and produce material that is promptly injected into the middle troposphere by winds. As outlined in Baccolo et al. (2018), conversely the typical alpine morphology that characterizes granitic nunataks, with pronounced peaks and steep cliffs, is less suitable for deflation and promotes accumulation of debris and glacial drift at the bottom of the walls, where deflation is disadvantaged.

Under these conditions, strong atmospheric uplift is not necessary in order to transport mineral aerosol to the site, while only the direction of air masses is important. Modern back trajectories reanalysis shows that dust transport from high-elevation ice-free areas of Victoria Land towards the Talos Dome area mainly occurs in spring/summer months and is mainly driven by local atmospheric circulation in the western Ross Sea, involving mesoscale cyclogenesis and northward-flowing air masses (Delmonte et al., 2013). Such a regional atmospheric circulation pattern involves only the margin of the East Antarctic ice sheet, as demonstrated by the limited spatial extent of local dust influence.

Interestingly, a steady feature of background dust at Talos Dome is the presence of geochemically-heterogeneous volcanic material, incompatible with derivation from a primary volcanic eruption (Delmonte et al., 2013). This volcanic contribution represents an intrinsic characteristic of the background dust at Talos Dome, suggesting a role played by wind in the secondary remobilization of volcanic material accumulated from different volcanic sources of Victoria Land. This volcanic contribution also accounts for the more volcanogenic isotopic fingerprint that characterizes the Holocene dust at Talos Dome if compared to the central plateau (figure 5) and for the peculiar ferromagnetic features of TALDICE Holocene dust (Lanci & Delmonte, 2013).

Similarly to Talos Dome, the radiogenic isotope and REE composition of dust in the Taylor Dome ice core (Aarons et al., 2016, Figure 5) also point towards a local dust provenance after the deglaciation and throughout the Holocene. Dust geochemical composition is characterized by a marked variability in time, in opposition to the homogeneous South American-like signature of dust from the last glacial period. A detailed study on dust from the Taylor Glacier (Aarons et al., 2017), originating from its accumulation area at Taylor Dome and terminating in the McMurdo Dry Valleys, confirms these findings and provides evidence that changes in local dust inputs occurred approximately concurrently to the Ross Ice Shelf retreat.

The documentation of the radiogenic isotope composition of dust and sandy sediments from Northern and Southern Victoria Land, as well as McMurdo Sound, was extended by Blakowski et al. (2016), that produced an interesting regional map showing the spatial variability of Sr and Nd isotopes in the area. The spatial patterns observed in the map are primarily related to parent lithologies (Beacon sandstone, Ferrar Dolerites, mixture of these with Kirkpatrick basalts and granites in some cases). Here we also integrate new Sr and Nd isotopic values of two moraine samples from Taylor Glacier (figure 5). As in the case of Talos Dome, however, the transport of volcanic material related to regional volcanic activity prevents any direct and definite source-to-sink comparison of isotopic signatures. From figure 5 it can be observed that some Holocene samples clearly fall within the Dry Valleys isotopic field, but the presence of volcanic material makes many Holocene data aligned towards a volcanic pole.

DUST CYCLE IN LOW ELEVATION ICE-FREE AREAS OF EAST ANTARCTICA

A number of ice free sites and other potential source of dust exist at low-elevation across East Antarctica; they consist of raised beaches, coastal oases and islands, cliffs and ice-free valleys, Late Pleistocene glacial drift and supraglacial debris on ice shelves (debris bands, Fig. 6A, 6B). Here we highlight their importance either as dominant source locally, or as potential contributors for atmospheric background dust at present day and in the past.

There is little information on transport distance of dust from proximal ice-free sources around the margin of Antarctica, and future work is required to understand the dust cycle on the margin of the ice sheet throughout the Holocene.

McMURDO SOUND

The McMurdo Sound is the dustiest known location in Antarctica. The dust accumulation there is spatially and temporally variable: the present-day dust flux is in the order of ~1 g m^{-2} yr^{-1}, which is orders of magnitude greater than long-range transport of remote dust in the central plateau (Chewings et al., 2014; Winton et al., 2014). Additionally, a modal particle size in the fine sand range and geochemical affinity with local rocks, confirm a local dust provenance (Winton et al., 2016a; Winton et al., 2014). Geochemistry and sedimentological studies of dust deposited on snow on McMurdo Sound sea ice (figure 6C) demonstrate that dust is locally-sourced from the debris bands on the McMurdo Ice Shelf. The debris bands (figure 6A) comprise an area of unconsolidated sediment, whereby sediment is lifted from the sea floor by anchor ice and frozen into the base of the ice shelf and eventually exposed by surface ablation (Kellogg et al., 1990). As such, the debris bands are considered to be an effectively unlimited source of aeolian dust (Atkins and Dunbar, 2009).

A progressive decrease in dust flux (55 to ~0.2 g m^{-2} yr^{-1}) and modal particle size (primary mode: 130 to 25 µm; fine silt mode relatively constant between 4-10 µm) has been observed along a dust plume extending >120 km northwards of the debris bands onto the sea ice (Atkins and Dunbar, 2009; Chewings et al., 2014; Winton et al., 2014; Macpherson, 1987). Dust dispersal northwards onto the sea ice is consistent with the local meteorology, since the fastest and most common winds that can entrain fine sand and silt, are predominantly from the South (katabatic flow). A local source for the supraglacial debris found on McMurdo ice shelf, is confirmed by Al/Fe elemental ratios (Atkins and Dunbar, 2009; De Jong et al., 2013) and Sr-Nd radiogenic isotopes (Winton et al., 2016a). The Sr and Nd isotopic composition of dust deposited along the sea ice dust plume (Winton et al., 2016a; Winton et al., 2014) forms a linear array resulting from a two component mixture of the isotopically-distinct McMurdo Volcanic Group ($0.703<^{87}Sr/^{86}Sr<0.710$; $-0.17<\varepsilon_{Nd}(0)<5.7$) and southern Victoria Land ($0.708<^{87}Sr/^{86}Sr<0.740$; $-12.5<\varepsilon_{Nd}(0)<-2.0$) (Delmonte et al., 2004, 2010b, 2013; Blakowski et al., 2016) end members. Despite the significant spatial variability in the region, dust on the McMurdo Sound sea ice represents the isotopic signature of McMurdo Sound (Winton et al., 2016a) that can be uplifted and transported to other Antarctic sites. The isotopic composition of McMurdo Sound dust source (figure 5) confirms, not surprisingly, that sediments are dominated by volcanogenic material.

Secondary elevated patches of dust occur within embayments and near coastal headlands along the south Victoria Land coastline. Sourced from the McMurdo Dry Valleys, the dust is not widely dispersed and thus the McMurdo Dry Valleys represent only a minor source of dust to the sea ice (Bentley, 1979; Barrett et al., 1983; Chewings et al., 2014; Winton et al., 2016a; Winton et al., 2014; Ayling and McGowan, 2006).

Ice-core records of dust accumulation in the McMurdo Sound region only span the past 35 years, where higher dust fluxes in winter are related to more frequent local storms (Ayling and McGowan, 2006; Dunbar et al., 2009). This region represented a local Antarctic low elevation dust source over the Pleistocene and the entire Holocene, since it has been ice-free for millions of years (Sugden et al., 1995). Dust accumulation measurements up to 120 km from the debris bands highlight that McMurdo Sound represents an important source of dust for the immediate southwestern Ross Sea area today (Winton et al., 2016a). However, while the large fraction dust flux is comprised of coarse-grained particles with limited transport distance, the still-unknown transport distance of the finer-grained particles potentially extends far beyond.

DRONNING MAUD LAND

Dronning Maud Land (DML) is located in the Weddell Sea sector of East Antarctica, directly downwind of the South American continent. Large drainage systems divide DML into an eastern, a central and a western part. Although the majority of DML is covered by ice, some outcrop massifs occur in this region: Heimefrontfjella and Vestfjella, Kirwanveggen and Mühlig-Hofmann

Mountains, Schirmacheroase, Steingarden and SørRondane Mountains, and Yamato-Belgica mountains. Their morphology resembles typical alpine landscapes, with U-shaped and hanging valleys that indicate a glacial origin, related to ancient wet-based glaciations (Holmlund & Näslund, 1994). These mountain ranges and nunataks represent important ice-free lands in DML.

Heimefrontfjella (10-13°W, 74-75°S) and Vestfjella (13-16°W, 73-74°S) are two important ranges of nunataks about 150 km apart, trending nearly parallel to the coastline. Heimefrontfjella, composed of various gneisses and schists of Precambrian age, represents an effective barrier to the ice flow, which is channeled in several outlet glaciers. Vestfjella, conversely, is a range of basaltic nunataks situated about 120 km from the coast. Basen is the northernmost nunatak, while nearby ones are Plogen and Fossilryggen. This latter is the only nunatak where Permian sedimentary rocks outcrop through the ice.

Here we present new Sr and Nd isotopic data (figure 7A) of: (1) regolith from the Vestfjella mountain range in DML and (2) ice core dust from a 100 m deep ice core that was drilled 140 km from the coast in the Vestfjella at Camp Maudheimvidda (CM, 73°06'19''S, 13°09'54´´W; 360 m a.s.l) during 1997-1998 as part of the EPICA pre-site survey. The site is within tens of kilometres of the Basen, Plogen and Fossilriyggen nunataks, and ~200 km north of Svea Station. Dating of the CM core shows that it covers a period from AD 1997-1700 (Jonsell et al., 2005). Two dust samples were extracted from the ice core sections: sample DML#1 represents the upper 55 m of the core, that at this depth consists of firn, its age spans 30-100 years before 1997; DML#2 was prepared extracting the dust from the lower part of the core, from 55 to 105 m depth, it roughly covers the time period between AD 1890 and 1790. The dust samples from both the CM ice core and the Basen, Ploggen and Fossilryggen nunataks, display a similar isotopic composition, restricted in a relatively narrow interval ($0.710378<{}^{87}Sr/{}^{86}Sr<0.715801$ and $-7.3<\varepsilon_{Nd}(0)<-8.5$). This interval is more restricted than bulk rock values from the area (Vestfjella basalts, andesites and tholeiites, Coats Land dolerites), and less radiogenic in Sr with respect to samples from the Svea station, where lithologies are different (granites, gneiss).

Besides indicating that dust at CM is locally-sourced, these data allow us to fingerprint the isotopic composition of this local, low-elevation area within DML. Isotopic values from CM ice core are distinctly different from values registered in central East Antarctica during pre-industrial times (figure 4, Delmonte et al., 2013), which represents the pristine remote input to the polar plateau, and can be useful to assess the regional importance of local dust transport even in more inland areas. So far, no radiogenic Sr and Nd isotope fingerprint exist for Holocene ice core dust from the

EPICA DML ice core drilled at Kohnen station (0° 04'E, 75°00'S) at about 2882 m a.s.l. However, Wegner et al. (2012), by using REE patterns, identified a clear contribution from multiple sources during the Holocene and generally after 15 ka BP. Surely, the high dust flux (figure 2) and atmospheric nssCa^{2+} concentration at the site, used as a proxy for mineral dust (Fischer et al., 2007), can be partly explained with the greater proximity of the South American dust source to the EPICA DML site. However, the possibility of a contribution from other sources must be also taken into account, as suggested by Wegner et al. (2015) on the basis of the phasing between dust emission and transport. The local importance of the contribution from Antarctic sources in the DML area can be also appreciated when considering the very high dust flux of 30-120 mg m^{-2} yr^{-1} registered for the last 50 years in a low elevation coastal ice core (IND-25/B5; 1300 m a.s.l., 71° 20' S, 11° 35' E), that is orders of magnitude higher than on the plateau (Laluraj et al., 2014).

BUNGER HILLS

Bunger Hills (Queen Mary Land; 66°S; 100°E; 165 m a.s.l.), also known as the Bunger Hills Oasis, is a low elevation ice free area of about 950 km^2 composed of a southern landmass and several large islands and marine inlets to the north. The Bunger Hills emerged from the ice sheet during the latest Pleistocene and early Holocene, and according to Augustinus et al. (1997) the Bunger Hills and the adjacent Islands to the west might have been ice-free throughout the Last Glacial Maximum. This seems corroborated by sand luminescence and radiocarbon dating described in Gore et al. (2001) and Augustinus and Duller (2002) (Table 1). The area consists of granulite-facies metamorphic rocks with a variety of compositions intruded by voluminous plutonic rocks (from gabbro to granite), and a variety of mafic dykes (Stüwe and Powell, 1989; Stüwe and Wilson, 1990; Sheraton et al., 1992; Ravich et al., 1968). The geochemistry of Bunger Hills rocks is described by Sheraton et al. (1993). In this work we document for the first time the Sr and Nd isotopic composition of some Bunger Hills fossil beach ridges of Holocene age (except one sample from the last glacial maximum), representing a low elevation potential source for dust since the last glacial period. Details about the samples, including their age, are reported in the supplementary material. Results are plotted in figure 7B. The isotopic range spanned by these samples ($0.720<{}^{87}Sr/{}^{86}Sr<0.761$ and $-24.3<\varepsilon_{Nd}(0)<-19.7$) is very similar to one moraine sample from Bunger Hills reported by Basile et al. (1997) and distinctly different from other Antarctic sources. Also, these values show no similarity with coeval dust archived in central East Antarctic ice cores, confirming that the Bunger Hills ice-free area has only a local relevance with respect to the atmospheric dust emission and deposition. These data will be useful for future studies aimed at assessing the regional dust cycle in the area during the late Quaternary.

CONCLUSIONS

The Holocene dust cycle in East Antarctica shows regional differences between high-altitude sites of the central East Antarctic plateau, marginal Victoria Land locations close to the Transantarctic Mountains, and low elevation coastal sites. The former display the lowest dust deposition fluxes on Earth, given the long atmospheric transport from remote, extra-Antarctic sources. High accuracy measurements have provided evidence that the grain size of mineral dust displays some variations on secular and decadal timescale, although it is always very small. This can be associated to variable atmospheric circulation patterns including the varying strength of air subsidence over Antarctica. Aeolian dust reaching these remote sites represents the well-mixed atmospheric background of the Southern Hemisphere. Given the extremely reduced contribution from remote sources, the Holocene dust history at the margin of the polar Plateau close to the Transantarctic Mountains, becomes sensitive to regional climate changes. While field evidences suggest that the areal extent of ice-free areas at high elevation (mountain tops, nunataks) did not change drastically since the last glacial maximum, the atmospheric circulation changes related also to the opening of the Ross Sea, surely played a role on local dust dispersal to the margin of the plateau during the Holocene. The contribution from patchy, low elevation sites of marginal East Antarctica is much less studied, except for the southwestern Ross Sea, the dustiest known place in Antarctica, where the so-called "debris bands" on the McMurdo ice shelf are found. Detailed studies in other sectors of the continent (DML, Bunger Hills, etc.) are presented, but need further investigation in order to assess the contribution of these sites to the atmospheric dust load over the Continent and the Southern Ocean.

Acknowledgments

This paper is a contribution to the Franco-Italian project SOLARICE (IPEV1145, PNRA16_00008). The field work at Concordia benefited from logistical support from the French and Italian Polar Agencies, IPEV and PNRA, and the C2FN for drilling activities.

BD acknowledges the SYNTHESYS SE-TAF-5636 project; HW acknowledges the “Friends of the Museum” Grant. This article is an outcome of Project “MIUR-Dipartimenti di Eccellenza 2018–2022”. We all acknowledge P. Augustinus for providing raised beach deposit samples from Bunger Hills and P. Biscaye for providing samples from Dronning Maud Land.

Tables and figure captions

Table 1: Ice core drilling sites with coordinates and age of the dust record considered, average dust concentration (ppb) for the time period indicated with standard deviation, average accumulation rate expressed in cm of water equivalent per year deduced from the AICC2012 timescale, average dust flux calculated from dust concentration and accumulation at each site, expressed in mg of dust per m^2 per year, altitude of each site and references for dust data.

Figure 1: Map of Antarctica with zoom on the McMurdo Sound area, Bunger Hills and Dronning Maud Land. The location of the most important ice core drilling sites cited in the text is indicated with a blue star. Toponyms are abbreviated as follows: EDC: EPICA Dome C; VK: Vostok; DB: Dome B; DF: Dome Fuji; TD: Talos Dome; TY:Taylor Dome; TG: Taylor Glacier; CM: Camp Maudheimvidda; EDML: EPICA Dronning Maud Land.

Figure 2: Early Holocene (11.7-8.2 kyr BP), Middle Holocene (8.2-4.2 kyr BP) and Late Holocene (4.2-2 kyr BP) dust flux (particles ø<5 µm) measured in seven different ice cores located on the East Antarctic plateau. The blue circle refers to data from the new SOLARICE-Dome C ice core (see text). Black boxes refer to preindustrial levels (between about AD 1800 and 1400). See Table 1 for data references.

Figure 3: Holocene dust grain-size variability at Dome C. (A) discontinuous, low resolution record of coarse particle percent (CPP) from the EPICA DC ice core (Delmonte et al., 2005); (B) running average of CPP dust grain size index measured at high resolution (4-5 cm long samples) on the new SOLARICE ice core. The red

curve represents a low frequency smoothing of data. (C) SEM images reporting examples of Holocene particles in central East Antarctic ice. Scale bar=5 µm.

Figure 4: $^{87}Sr/^{86}Sr$ versus $\varepsilon_{Nd}(0)$ isotopic composition of East Antarctic ice core dust from the Holocene and from MIS2 and of fine sediments (S) and aeolian dust (AD) from potential source areas. Holocene ice core data are from Dome C and Vostok; MIS2 ice core data are from Dome C, Vostok, Dome B. One additional point for the previous interglacial (MIS 5.5) is also reported for comparison. Source data are referred to the fine fraction of aeolian dust (AD) and sediments (S) of different typology (topsoil, loess, alluvial fans, ephemeral lakes, lacustrine clay/silt, fluvial suspended load, salar edges, etc.) from South America, Australia and New Zealand. Data from the Illimani ice core (Bolivian Altiplano, 16°37'S, 67°46'W) are also reported for comparison.

Data sources: Basile et al., 1997; Delmonte et al., 2004; 2007; 2010; 2013; 2017; Smith et al., 2003; Gaiero, 2007; Gaiero et al., 2004, 2007, 2013; Gili et al., 2017; Sugden et al., 2009; Revel-Rolland et al., 2006; Gingele and De Deckker 2005.

Figure 5: $^{87}Sr/^{86}Sr$ versus $\varepsilon_{Nd}(0)$ isotopic composition of Holocene and MIS2 ice core dust from marginal East Antarctic plateau sites in Northern and Southern Victoria land (Talos Dome, Delmonte et al., 2010, 2013; Taylor Dome, Aarons et al., 2016) **and Taylor Glacier** (Aarons et al., 2017).

Ice-core data are compared with fine sediments from local Antarctic dust sources (Blakowski et al., 2016; Delmonte et al., 2010, 2013, Winton et al., 2014, 2016a, 2016b, and this work), bulk rocks (Fleming et al., 1992, 1995) and the volcanic end-member (Rocholl et al., 1995). The black ellipse highlights the isotopic field for McMurdo Sound dust identified by Winton et al., 2016a. The two black circles refer to new data from the Dry Valleys analyzed in this work (see text and supplementary material).

Figure 6: (**6A**) **Late Peistocene glacial drift** (in foreground) with granite erratic (white) on Bratina Is. and supraglacial debris band on McMurdo Ice Shelf (in background). (**6B**) **Section** in the Late Pleistocene glacial drift (younger drift) on the Dailey Island West. Note the aeolian deflation pavement on top. **(6C) Southern McMurdo Sound**, November 2009: snow on sea ice sampling for dust provenance studies. Photo credit: James Pinchin.

Fig. 7: Sr-Nd isotopic composition of Holocene ice core dust from low elevations sites. (A) Camp Maudheimvidda (CM) ice core in coastal DML, local nunataks (Basen, Ploggen, Fossilryggen) and Svea station. Isotopic fields are drawn from literature data on bulk rocks (basalts, tholeiites, andesites) from the DML area of Vestfjella, and Coats Land dolerites (Luttinen & Furnes, 2000; Harris et al., 1990; Riley et al., 2005; Brewer et al., 1992). (B) **Bunger Hills**. Sr-Nd isotopic data from bulk (all size included) and fine (<5

μm) dust samples from the Bunger Hills raised beaches in Wilkes Land (see text) as well as one data point from a local moraine (Basile et al. 1997).

References

Aarons SM, Aciego SM, Arendt CA et al (2017) Dust composition changes from Taylor Glacier (East Antarctica) during the last glacial-interglacial transition: A multi-proxy approach. *Quaternary Science Reviews*, *162*, 60-71.

Aarons SM, Aciego SM, Gabrielli P et al. (2016) The impact of glacier retreat from the Ross Sea on local climate: Characterization of mineral dust in the Taylor Dome ice core, East Antarctica. *Earth and Planetary Science Letters*, *444*, 34-44.

Albani S, Delmonte B, Maggi V, et al. (2012) Interpreting last glacial to Holocene dust changes at Talos Dome (East Antarctica): implications for atmospheric variations from regional to hemispheric scales. *Climate of the Past*, *8*, 741-750.

Atkins CB & Dunbar GB (2009) Aeolian sediment flux from sea ice into Southern McMurdo Sound, Antarctica, Global and Planetary Change, 69, 133-141, 2009.

Augustinus PC, Gore DB, Leishman MR et al (1997) Reconstruction of ice flow across the Bunger Hills, East Antarctica. *Antarctic Science*, *9*(3), 347-354.

Augustinus P & Duller G (2002) Luminescence and radiocarbon dating of raised beach sediments, Bunger Hills, East Antarctica, Antarctica at the close of a millennium: proceedings of the 8th International Symposium on Antarctic Earth Sciences, Wellington.

Ayling BF & McGowan HA (2006) Niveo-eolian sediment deposits in coastal South Victoria Land, Antarctica: indicators of regional variability in weather and climate, Arctic, Antarctic, and Alpine Research, 38, 313-324.

Baccolo G, Delmonte B, Albani S et al. (2018) Regionalization of the atmospheric dust cycle on the periphery of the East Antarctic ice sheet since the last glacial maximum. *Geochemistry, Geophysics, Geosystems*.

Baroni, C., Frezzotti, M., Salvatore, M. C., Meneghel, M., Tabacco, I. E., Vittuari, L., et al. (2004). Antarctic geomorphological and glaciological 1:250 000 map series: Mount Murchison quadrangle, northern Victoria Land. Explanatory notes. Annals of Glaciology, 39, 256–264.

Barrett P, Pyne A and Ward B (1983) Modern sedimentation in McMurdo Sound, Antarctica In: Oliver, R.L., James, P.R., Jago, J.B. (Eds.), Australian Academy of Sciences, Canberra, 550-554.

Basile I, Grousset FE, Revel M et al. (1997) Patagonian origin of glacial dust deposited in East Antarctica (Vostok and Dome C) during glacial stages 2, 4 and 6. *Earth and Planetary Science Letters*, *146*(3-4), 573-589.

Bentley P (1979) Characteristics and distribution of wind blown sediments, Western McMurdo Sound, Antarctica, Bachelor of Science Honours thesis, School of Earth Sciences, Victoria University of Wellington, Wellington.

Blakowski MA, Aciego SM, Delmonte B et al. (2016). A Sr-Nd-Hf isotope characterization of dust source areas in Victoria Land and the McMurdo Sound sector of Antarctica. *Quaternary Science Reviews*, *141*, 26-37.

Brewer TS, Hergt JM, Hawkesworth CJ et al. (1992) Coats Land dolerites and the generation of Antarctic continental flood basalts. *Geological Society, London, Special Publications*, *68*(1), 185-208. *Chemical Geology*, *238*(1-2), 107-120.

Chewings J, Atkins C, Dunbar G et al. (2014) Aeolian sediment transport and deposition in a modern high latitude glacial marine environment, Sedimentology.

De Deckker P, Norman M, Goodwin ID et al. (2010). Lead isotopic evidence for an Australian source of aeolian dust to Antarctica at times over the last 170,000 years. *Palaeogeography, Palaeoclimatology, Palaeoecology*, *285*(3-4), 205-223.

De Jong J, Schoemann V, Maricq N et al. (2013) Iron in land-fast sea ice of McMurdo Sound derived from sediment resuspension and wind-blown dust attributes to primary productivity in the Ross Sea, Antarctica, Marine Chemistry, 157, 24-40.

Delmonte B, Petit JR & Maggi V (2002) Glacial to Holocene implications of the new 27000-year dust record from the EPICA Dome C (East Antarctica) ice core. *Climate Dynamics*, *18*(8), 647-660.

Delmonte B (2003) Quaternary origin and variations of continental dust in East Antarctica. Diss. Ph. D Thesis, University of Siena (Italy), Universite Joseph Fourier-Grenoble I, Grenoble (France).

Delmonte B, Basile-Doelsch I, Petit JR et al. (2004). Comparing the Epica and Vostok dust records during the last 220,000 years: stratigraphical correlation and provenance in glacial periods. *Earth-Science Reviews*, *66*(1-2), 63-87.

Delmonte B, Petit JR, Krinner G et al. (2005). Ice core evidence for secular variability and 200-year dipolar oscillations in atmospheric circulation over East Antarctica during the Holocene. *Climate dynamics*, *24*(6), 641-654.

Delmonte B, Petit JR, Basile-Doelsch I et al. (2007). Late quaternary interglacials in East Antarctica from ice-core dust records. In *Developments in Quaternary Sciences* (Vol. 7, pp. 53-73). Elsevier.

Delmonte B, Andersson PS, Hansson M et al. (2008). Aeolian dust in East Antarctica (EPICA-Dome C and Vostok): Provenance during glacial ages over the last 800 kyr. *Geophysical Research Letters*, *35*(7).

Delmonte B, Andersson PS, Schöberg H et al. (2010a). Geographic provenance of aeolian dust in East Antarctica during Pleistocene glaciations: preliminary results from Talos Dome and comparison with East Antarctic and new Andean ice core data. *Quaternary Science Reviews*, *29*(1-2), 256-264.

Delmonte B, Baroni C, Andersson PS et al. (2010b). Aeolian dust in the Talos Dome ice core (East Antarctica, Pacific/Ross Sea sector): Victoria Land versus remote sources over the last two climate cycles. *Journal of Quaternary Science*, *25*(8), 1327-1337.

Delmonte B, Baroni C, Andersson PS et al. (2013). Modern and Holocene aeolian dust variability from Talos Dome (Northern Victoria Land) to the interior of the Antarctic ice sheet. *Quaternary Science Reviews*, *64*, 76-89.

Delmonte B, Paleari CI, Andò S et al. (2017). Causes of dust size variability in central East Antarctica (Dome B): Atmospheric transport from expanded South American sources during Marine Isotope Stage 2. *Quaternary Science Reviews*, *168*, 55-68.

Di Nicola L, Baroni C, Strasky S et al. (2012) Multiple cosmogenic nuclides document the stability of the East Antarctic Ice Sheet in northern Victoria Land since the Late Miocene (5-7 Ma). Quaternary Science Reviews, 57, 85-94.

Du Z, Xiao C, Ding M et al. (2018). Identification of multiple natural and anthropogenic sources of dust in snow from Zhongshan Station to Dome A, East Antarctica. *Journal of Glaciology*, 1-11.

Dunbar GB, Bertler NAN & McKay RM (2009) Sediment flux through the McMurdo Ice Shelf in Windless Bight, Antarctica, Global and Planetary Change, 69, 87-93.

Duprat J, Engrand C, Maurette M et al. (2007). Micrometeorites from central Antarctic snow: The CONCORDIA collection. Advances in Space Research, 39(4), 605-611.

Fischer H, Fundel F, Ruth U et al. (2007). Reconstruction of millennial changes in dust emission, transport and regional sea ice coverage using the deep EPICA ice cores from the Atlantic and Indian Ocean sector of Antarctica. *Earth and Planetary Science Letters*, *260*(1), 340-354.

Fleming TH, Elliot DH, Jones LM et al. (1992) Chemical and isotopic variations in an iron-rich lava flow from the Kirkpatrick Basalt, north Victoria Land, Antarctica: implications for low-temperature alteration. *Contributions to Mineralogy and Petrology*, *111*(4), 440-457.

Fleming TH, Foland KA & Elliot DH (1995) Isotopic and chemical constraints on the crustal evolution and source signature of Ferrar magmas, north Victoria Land, Antarctica. *Contributions to Mineralogy and Petrology*, *121*(3), 217-236.

Fujii Y & Ohata T (1982) Possible causes of the variation in microparticle concentration in an ice core from Mizuho Station, Antarctica. Ann. Glaciol., 3, 107–112.

Fujii Y, Kohno M, Matoba S et al. (2003). A 320 k-year record of microparticles in the Dome Fuji, Antarctica ice core measured by laser-light scattering.

Gabrielli P, Wegner A, Petit JR et al. (2010). A major glacial-interglacial change in aeolian dust composition inferred from Rare Earth Elements in Antarctic ice. *Quaternary Science Reviews*, *29*(1-2), 265-273.

Gaiero DM, Depetris PJ, Probst JL et al. (2004) The signature of river-and wind-borne materials exported from Patagonia to the southern latitudes: a view from REEs and implications for paleoclimatic interpretations. Earth and Planetary Science Letters, 219(3-4), 357-376.

Gaiero DM (2007) Dust provenance in Antarctic ice during glacial periods: from where in southern South America? *Geophysical Research Letters*, *34*(17).

Gaiero DM, Brunet F, Probst JL et al. (2007) A uniform isotopic and chemical signature of dust exported from Patagonia: Rock sources and occurrence in southern environments.

Gaiero DM, Simonella L, Gassó S et al. (2013) Ground/satellite observations and atmospheric modeling of dust storms originating in the high Puna-Altiplano deserts (South America): Implications for the interpretation of paleo-climatic archives. Journal of Geophysical Research: Atmospheres, 118(9), 3817-3831.

Gaudichet A, De Angelis M, Lefevre R et al. (1988) Mineralogy of insoluble particles in the Vostok Antarctic ice core over the last climatic cycle (150 kyr). *Geophysical Research Letters*, *15*(13), 1471-1474.

Gaudichet A, Petit JR Lefevre R et al. (1986) An investigation by analytical transmission electron microscopy of individual insoluble microparticles from Antarctic (Dome C) ice core samples. *Tellus B*, *38*(3-4), 250-261.

Gaudichet A, Petit JR, Lefevre R et al. (1986) An investigation by analytical transmission electron microscopy of individual insoluble microparticles from Antarctic (Dome C) ice core samples. *Tellus B*, *38*(3-4), 250-261.

Genthon C & Armengaud A (1995) Radon 222 as a comparative tracer of transport and mixing in two general circulation models of the atmosphere. *Journal of Geophysical Research: Atmospheres*, *100*(D2), 2849-2866.

Gili S, Gaiero DM, Goldstein S et al. (2017) Glacial/interglacial changes of Southern Hemisphere wind circulation from the geochemistry of South American dust. *Earth and Planetary Science Letters*, *469*, 98-109.

Gili S, Gaiero DM, Goldstein S et al. (2016) Provenance of dust to Antarctica: A lead isotopic perspective. *Geophysical Research Letters*, *43*(5), 2291-2298.

Gingele FX & De Deckker P (2005) Clay mineral, geochemical and Sr–Nd isotopic fingerprinting of sediments in the Murray–Darling fluvial system, southeast Australia. *Australian Journal of Earth Sciences*, *52*(6), 965-974.

Gore DB, Rhodes EJ, Augustinus PC et al. (2001) Bunger Hills, East Antarctica: ice free at the last glacial maximum. *Geology*, *29*(12), 1103-1106.

Grousset F, Biscaye P, Revel M et al. (1992) Antarctic (Dome C) ice-core dust at 18 ky BP: Isotopic constraints on origins, *Earth and Planetary Science Letters, 111*, 175-182.

Harris C, Marsh JS, Duncan AR et al. (1990) The petrogenesis of the Kirwan Basalts of Dronning Maud Land, Antarctica. *Journal of Petrology*, *31*(2), 341-369.

Holmlund P & Näslund JO (1994) The glacially sculptured landscape in Dronning Maud Land, Antarctica, formed by wet-based mountain glaciation and not by the present ice sheet. *Boreas, 23*, 139-148.

Iriondo MH (1997) Models of deposition of loess and loessoids in the Upper Quaternary of South America. *Journal of South American Earth Sciences, 10*(1), 71-79.

Jacob DJ , Prather MJ, Boville BA et al. (1997) Intercomparison of convective and synoptic transport in global models using 222Rn and other tracers. *J. Geophys. Res*, *102*, 5953.

Jonsell U, Hansson M, Morth CM et al. (2005) Sulfur isotopic signals in two shallow ice cores from Dronning Maud Land, Antarctica, Tellus B, 57, 341-350, 10.1111/j.1600-0889.2005.00157.x.

Kawamura K, Abe-Ouchi A, Motoyama H et al. (2017). State dependence of climatic instability over the past 720,000 years from Antarctic ice cores and climate modeling. Science advances, 3(2), e1600446.

Kellogg TB, Kellogg D & Stuiver M (1990) Late Quaternary History of the Southwestern Ross Sea: Evidence from Debris Bands on the McMurdo Ice Shelf, Antarctica, Antarctic Res. Ser. (AGU), 50, 25-56.

Krinner G & Genthon C (2003) Tropospheric transport of continental tracers towards Antarctica under varying climatic conditions. *Tellus, 55B*, 54-70.

Laluraj CM, Thamban M and Satheesan K (2014) Dust and associated geochemical fluxes in a firn core from coastal East Antarctica and its linkages with Southern Hemisphere climate varaibility over the last 50 years. *Atmospheric Envionment, 90*, 23-32.

Lambert F, Delmonte B, Petit JR et al. (2008) Dust-climate couplings over the past 800,000 years from the EPICA Dome C ice core. *Nature*, *452*(7187), 616.

Lanci L, Delmonte B, Maggi V et al. (2008) Ice magnetization in the EPICA-Dome C ice core: Implication for dust sources during glacial and interglacial periods. *Journal of Geophysical Research: Atmospheres*, *113*(D14).

Lanci L, Delmonte B, Kent DV et al. (2012) Magnetization of polar ice: a measurement of terrestrial dust and extraterrestrial fallout. Quaternary Science Reviews, 33, 20-31.

Lanci L & Delmonte B (2013) Magnetic properties of aerosol dust in peripheral and inner Antarctic ice cores as a proxy for dust provenance. Global and planetary change, 110, 414-419.

Legrand M & Mayewski P (1997) Glaciochemistry of polar ice cores: a review. *Reviews of geophysics*, *35*(3), 219-243.

Li F, Ginoux P & Ramaswamy V (2008) Distribution, transport, and deposition of mineral dust in the Southern Ocean and Antarctica: Contribution of major sources. *Journal of Geophysical Research: Atmospheres*, *113*(D10).

Luttinen AV & Furnes H (2000) Flood basalts of Vestfjella: Jurassic magmatism across an Archaean–Proterozoic lithospheric boundary in Dronning Maud Land, Antarctica. *Journal of Petrology*, *41*(8), 1271-1305.

Macpherson A (1987) The MacKay Glacier/Granite Harbour system (Ross Dependency, Antarctica). A study in nearshore glacial marine sedimentation, Victoria University of Wellington, Wellington, 85 pp.

Maenhaut W, Zoller WH & Coles DG (1979) Radionuclides in the south pole atmosphere.[1973--1975]. *J. Geophys. Res.;(United States)*, *84*(C6).

Marino F, Castellano E, Ceccato D et al. (2008). Defining the geochemical composition of the EPICA Dome C ice core dust during the last glacial-interglacial cycle. *Geochemistry, geophysics, geosystems*, *9*(10).

Markle BR, Steig EJ, Roe GH et al. (2018) Concomitant variability in high-latitude aerosols, water isotopes and the hydrological cycle. *Nature Geoscience*, DOI: 10.1038/s41561-018-0210-9.

Narcisi B, Petit JR, Delmonte B et al. (2005) Characteristics and sources of tephra layers in the EPICA-Dome C ice record (East Antarctica): implications for past atmospheric circulation and ice core stratigraphic correlations. *Earth and Planetary Science Letters*, *239*(3), 253-265.

Neff PD & Bertler NAN (2015) Trajectory modeling of modern dust transport to the Southern Ocean and Antarctica. *Journal of Geophysical Research: Atmospheres*, 120(18), 9303-9322.

Oberholzer P, Baroni C, Salvatore MC et al. (2008). Dating late Cenozoic erosional surfaces in Victoria Land, Antarctica, with cosmogenic neon in pyroxenes. *Antarctic Science*, *20*(1), 89-98.

Oberholzer P, Baroni C, Schaefer JM (2003). Limited Pliocene/Pleistocene glaciation in Deep Freeze Range, northern Victoria Land, Antarctica, derived from in situ cosmogenic nuclides. *Antarctic Science*, *15*(4), 493-502.

Petit JR & Delmonte B (2009) A model for large glacial–interglacial climate-induced changes in dust and sea salt concentrations in deep ice cores (central Antarctica): palaeoclimatic implications and prospects for refining ice core chronologies. *Tellus B: Chemical and Physical Meteorology*, *61*(5), 768-790.

Petit JR, Briat M & Royer A (1981) Ice age aerosol content from East Antarctic ice core samples and past wind strength. Nature, 293(5831), 391.

Petit JR, Jouzel J, Raynaud D et al. (1999). Climate and atmospheric history of the past 420,000 years from the Vostok ice core, Antarctica. *Nature*, *399*(6735), 429.

Potenza MAC, Albani S, Delmonte B et al. (2016) Shape and size constraints on dust optical properties from the Dome C ice core, Antarctica. *Scientific reports*, *6*, 28162.

Ravich MG, Klimov L & Solov'ev D (1968) The Pre-Cambrian of East Antarctica, 51403, Israel Program for Scientific Translations.

Revel-Rolland M, De Deckker P, Delmonte B et al. (2006) Eastern Australia: a possible source of dust in East Antarctica interglacial ice. *Earth and Planetary Science Letters*, *249*(1-2), 1-13.

Riley TR, Leat PT, Curtis ML et al. (2005). Early–Middle Jurassic dolerite dykes from Western Dronning Maud Land (Antarctica): identifying mantle sources in the Karoo large igneous province. *Journal of Petrology*, *46*(7), 1489-1524.

Rocholl A, Stein M, Molzahn M et al. (1995) Geochemical evolution of rift magmas by progressive tapping of a stratified mantle source beneath the Ross Sea Rift, Northern Victoria Land, Antarctica. *Earth and Planetary Science Letters*, *131*(3-4), 207-224.

Ruth U, Wagenbach D, Bigler M et al. (2002) High-resolution microparticle profiles at NorthGRIP, Greenland: case studies of the calcium–dust relationship. Ann. Glaciol., 35 , 237–242.

Ruth U, Barbante C, Bigler M et al. (2008). Proxies and measurement techniques for mineral dust in Antarctic ice cores. *Environmental science & technology*, *42*(15), 5675-5681.

Sayago JM, Collantes MM, Karlson A et al. (2001) Genesis and distribution of the Late Pleistocene and Holocene loess of Argentina: a regional approximation. Quaternary International, 76, 247-257.

Sheraton JW, Black LP & Tindle AG (1992) Petrogenesis of plutonic rocks in a Proterozoic granulite-facies terrane — the Bunger Hills, East Antarctica, Chemical Geology, 97, 163-198, http://dx.doi.org/10.1016/0009-2541(92)90075-G.

Sheraton JW, Tingey RJ, Black LP et al. (1993) Geology of the Bunger Hills area, Antarctica: implications for Gondwana correlations, Antarctic Science, 5, 85-102, doi:10.1017/S0954102093000112.

Siggaard-Andersen ML, Gabrielli P, Steffensen JP et al. (2007). Soluble and insoluble lithium dust in the EPICA DomeC ice core—Implications for changes of the East Antarctic dust provenance during the recent glacial–interglacial transition. *Earth and planetary science letters*, *258*(1-2), 32-43.

Simonsen MF, Cremonesi L, Baccolo G et al. (2018) Particle shape accounts for instrumental discrepancy in ice core dust size distributions. Climate of the Past, 14(5), 601-608.

Smith J, Vance D, Kemp RA et al. (2003). Isotopic constraints on the source of Argentinian loess–with implications for atmospheric circulation and the provenance of Antarctic dust during recent glacial maxima. *Earth and Planetary Science Letters*, *212*(1-2), 181-196.

Stüwe K & Powell R (1989) Metamorphic evolution of the Bunger Hills, East Antarctica: evidence for substantial post-metamorphic peak compression with minimal cooling in a Proterozoic orogenic event, Journal of Metamorphic Geology, 7, 449-464, 10.1111/j.1525-1314.1989.tb00608.x.

Stüwe K & Wilson CJL (1990) Interaction between deformation and charnockite emplacement in the Bunger Hills, East Antarctica, Journal of Structural Geology, 12, 767-783, http://dx.doi.org/10.1016/0191-8141(90)90088-G.

Sugden DE, Marchant DR, Potter Jr N et al. (1995) Preservation of Miocene glacier ice in East Antarctica, Nature, 376, 412.

Sugden DE, McCulloch RD, Bory AJ et al. (2009) Influence of Patagonian glaciers on Antarctic dust deposition during the last glacial period. *Nature Geoscience*, *2*(4), 281.

Unnerstad L & Hansson M (2001) Simulated airborne particle size distributions over Greenland during Last Glacial Maximum. *Geophysical research letters*, *28*(2), 287-290.

Vallelonga P, Gabrielli P, Balliana E et al. (2010) Lead isotopic compositions in the EPICA Dome C ice core and Southern Hemisphere Potential Source Areas. *Quaternary Science Reviews*, *29*(1), 247-255.

Veres D, Bazin L, Landais A et al. (2013) The Antarctic ice core chronology (AICC2012): an optimized multi-parameter and multi-site dating approach for the last 120 thousand years. *Climate of the Past Discussions*, *8*(6).

Wegner A, Fischer H, Delmonte B et al. (2015) The role of seasonality of mineral dust concentration and size on glacial/interglacial dust changes in the EPICA Dronning Maud Land ice core, Journal of Geophysical Research: Atmospheres, 120, 9916-9931, 10.1002/2015JD023608.

Wegner A, Gabrielli P, Wilhelms-Dick D et al. (2012) Change in dust variability in the Atlantic sector of Antarctica at the end of the last deglaciation. *Climate of the Past*, *8*(1), 135-147.

Winton VHL, Dunbar GB, Bertler NAN et al. (2014) The contribution of aeolian sand and dust to iron fertilization of phytoplankton blooms in southwestern Ross Sea, Antarctica, Global Biogeochemical Cycles, 28, 2013GB004574, 10.1002/2013GB004574.

Winton VHL, Dunbar G, Atkins C et al. (2016a) The origin of lithogenic sediment in the south-western Ross Sea and implications for iron fertilization, Antarctic Science, 28, 250-260, 2016a.

Winton VHL, Edwards R, Delmonte B et al. (2016b) Multiple sources of soluble atmospheric iron to Antarctic waters, Global Biogeochemical Cycles, 30, 421-437, 10.1002/2015GB005265.

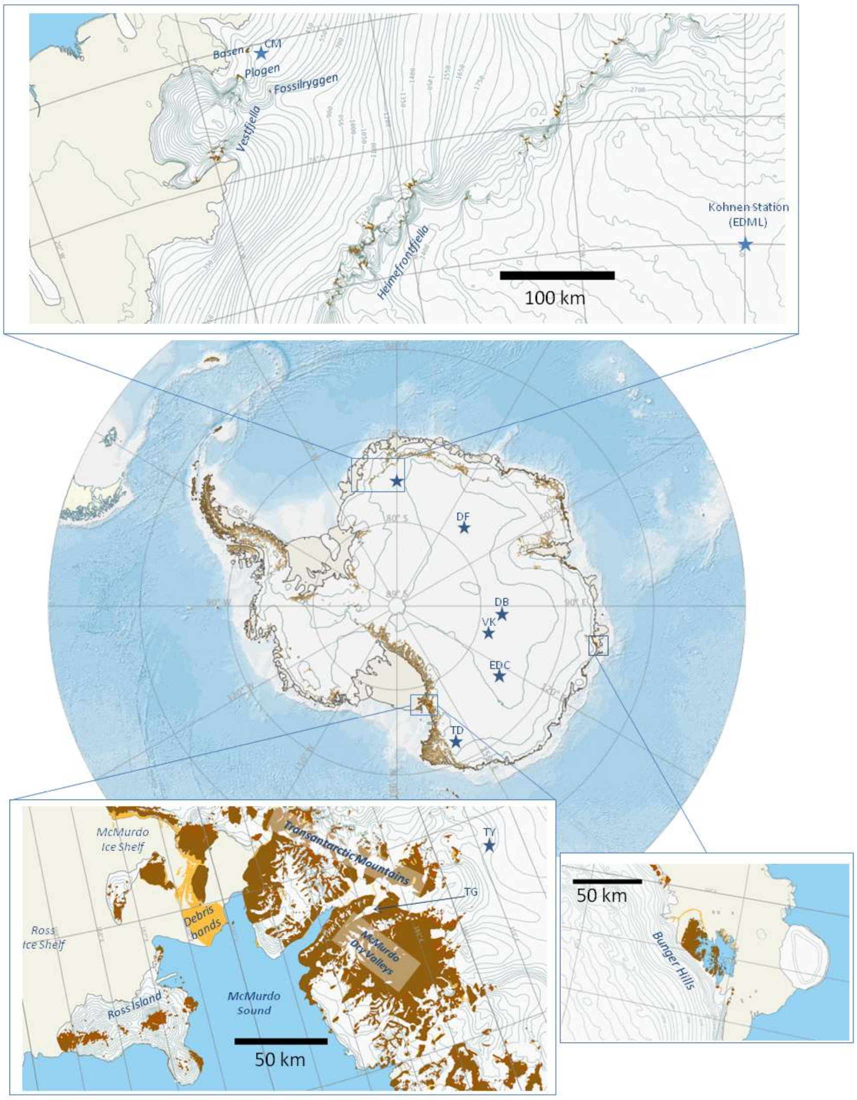

Figure 1: Map of Antarctica with zoom on the McMurdo Sound area, Bunger Hills and Dronning Maud Land. The location of the most important ice core drilling sites cited in the text is indicated with a blue star. Toponyms are abbreviated as follows: EDC: EPICA Dome C; VK: Vostok; DB: Dome B; DF: Dome Fuji; TD: Talos Dome; TY:Taylor Dome; TG: Taylor Glacier; CM: Camp Maudheimvidda; EDML: EPICA Dronning Maud Land.

266x355mm (96 x 96 DPI)

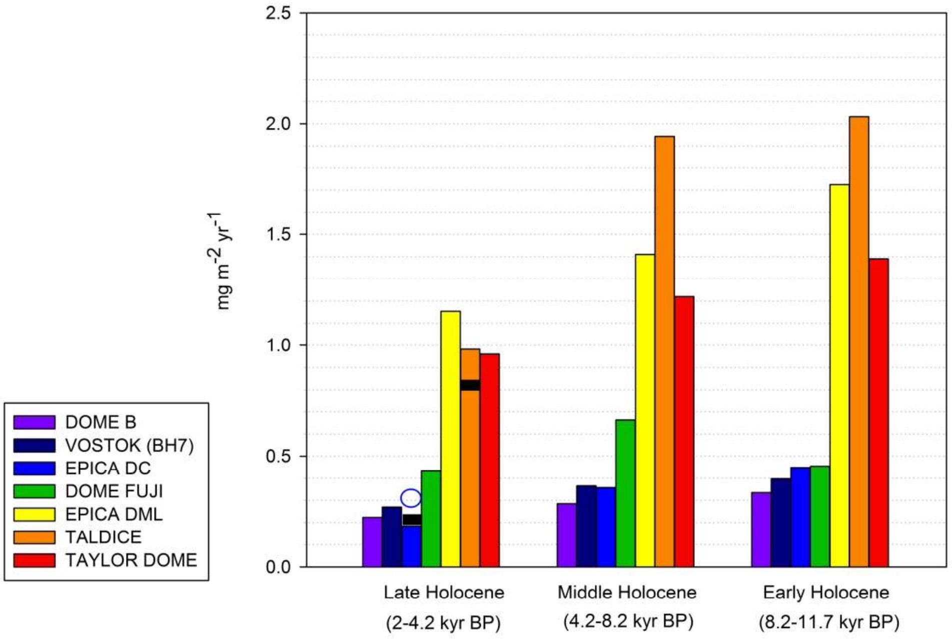

Figure 2: Early Holocene (11.7-8.2 kyr BP), Middle Holocene (8.2-4.2 kyr BP) and Late Holocene (4.2-2 kyr BP) dust flux (particles ø<5 μm) measured in seven different ice cores located on the East Antarctic plateau. The blue circle refers to data from the new SOLARICE-Dome C ice core (see text). Black boxes refer to preindustrial levels (between about AD 1800 and 1400). See Table 1 for data references.

256x181mm (300 x 300 DPI)

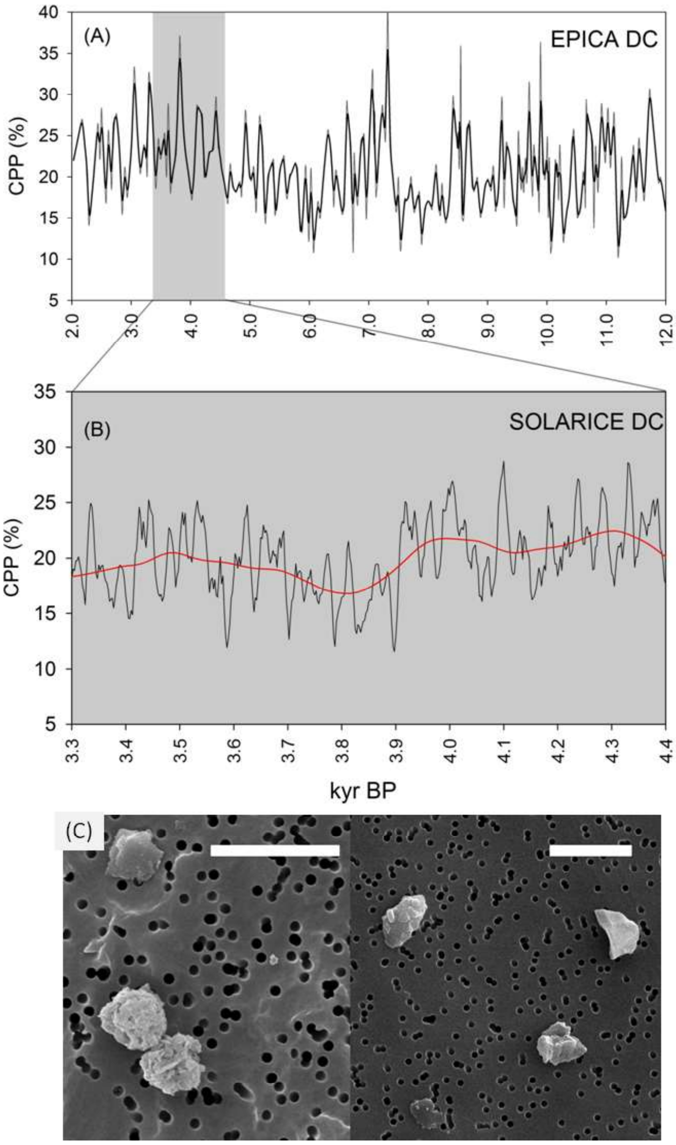

Figure 3: Holocene dust grain size variability at Dome C. (A) discontinuous, low resolution record of coarse particle percent (CPP) from the EPICA DC ice core (Delmonte et al., 2005); (B) running average of CPP dust grain size index measured at high resolution (4-5 cm long samples) on the new SOLARICE ice core. The red curve represents a low frequency smoothing of data. (C) SEM images reporting examples of Holocene particles in central East Antarctic ice. Scale bar=5 μm.

190x300mm (96 x 96 DPI)

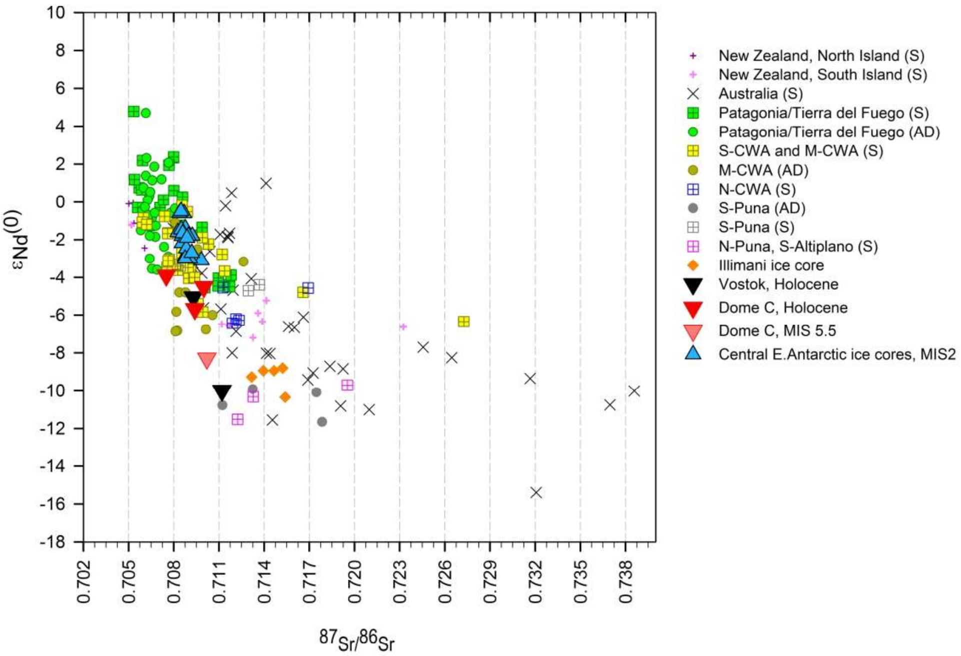

Figure 4: 87Sr/86Sr versus □Nd(0) isotopic composition of East Antarctic ice core dust from the Holocene and from MIS2 and of fine sediments (S) and aeolian dust (AD) from potential source areas. Holocene ice core data are from Dome C and Vostok; MIS2 ice core data are from Dome C, Vostok, Dome B. One additional point for the previous interglacial (MIS 5.5) is also reported for comparison. Source data are referred to the fine fraction of aeolian dust (AD) and sediments (S) of different typology (topsoil, loess, alluvial fans, ephemeral lakes, lacustrine clay/silt, fluvial suspended load, salar edges, etc.) from South America, Australia and New Zealand. Data from the Illimani ice core (Bolivian Altiplano, 16°37'S, 67°46'W) are also reported for comparison.
Data sources: Basile et al., 1997; Delmonte et al., 2004; 2007; 2010; 2013; 2017; Smith et al., 2003; Gaiero, 2007; Gaiero et al., 2004, 2007, 2013; Gili et al., 2017; Sugden et al., 2009; Revel-Rolland et al., 2006; Gingele and De Deckker 2005.

270x269mm (300 x 300 DPI)

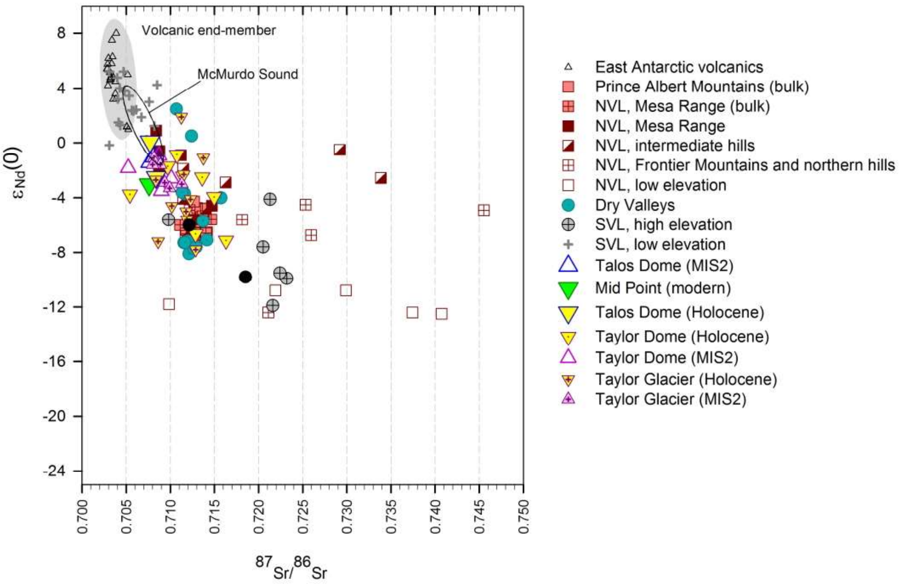

Figure 5: 87Sr/86Sr versus □Nd(0) isotopic composition of Holocene and MIS2 ice core dust from marginal East Antarctic plateau sites in Northern and Southern Victoria land (Talos Dome, Delmonte et al., 2010, 2013; Taylor Dome, Aarons et al., 2016) and Taylor Glacier (Aarons et al., 2017).
Ice-core data are compared with fine sediments from local Antarctic dust sources (Blakowski et al., 2016; Delmonte et al., 2010, 2013, Winton et al., 2014, 2016a, 2016b, and this work), bulk rocks (Fleming et al., 1992, 1995) and the volcanic end-member (Rocholl et al., 1995). The black ellipse highlights the isotopic field for McMurdo Sound dust identified by Winton et al., 2016a. The two black circles refer to new data from the Dry Valleys analyzed in this work (see text and supplementary material).

300x270mm (300 x 300 DPI)

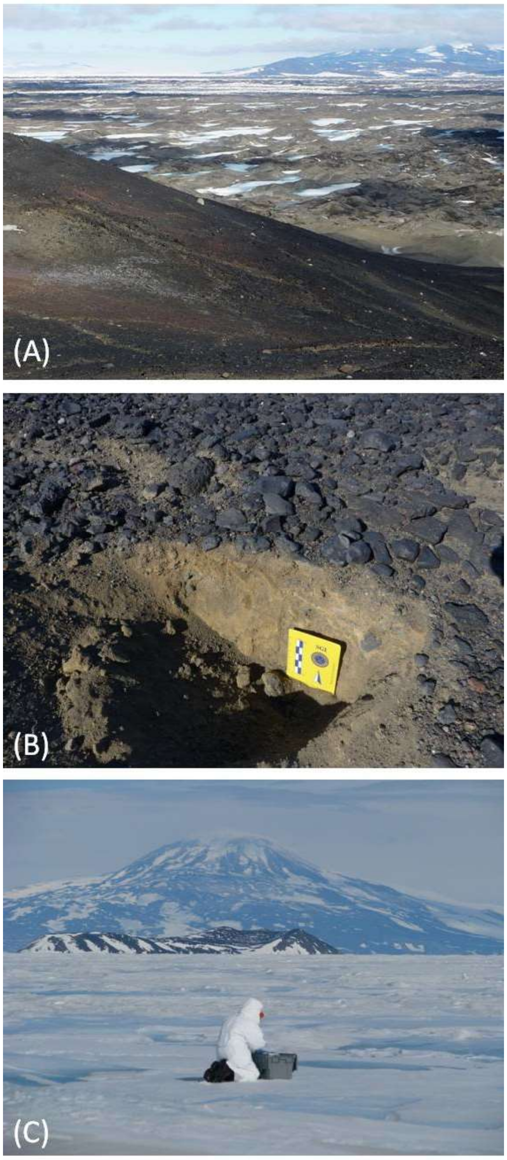

Figure 6: (6A) Late Peistocene glacial drift (in foreground) with granite erratic (white) on Bratina Is. and supraglacial debris band on McMurdo Ice Shelf (in background). (6B) Section in the Late Pleistocene glacial drift (younger drift) on the Dailey Island West. Note the eolic deflation pavement on top. (6C) Southern McMurdo Sound, November 2009: snow on sea ice sampling for dust provenance studies. Photo credit: James Pinchin.

150x350mm (96 x 96 DPI)

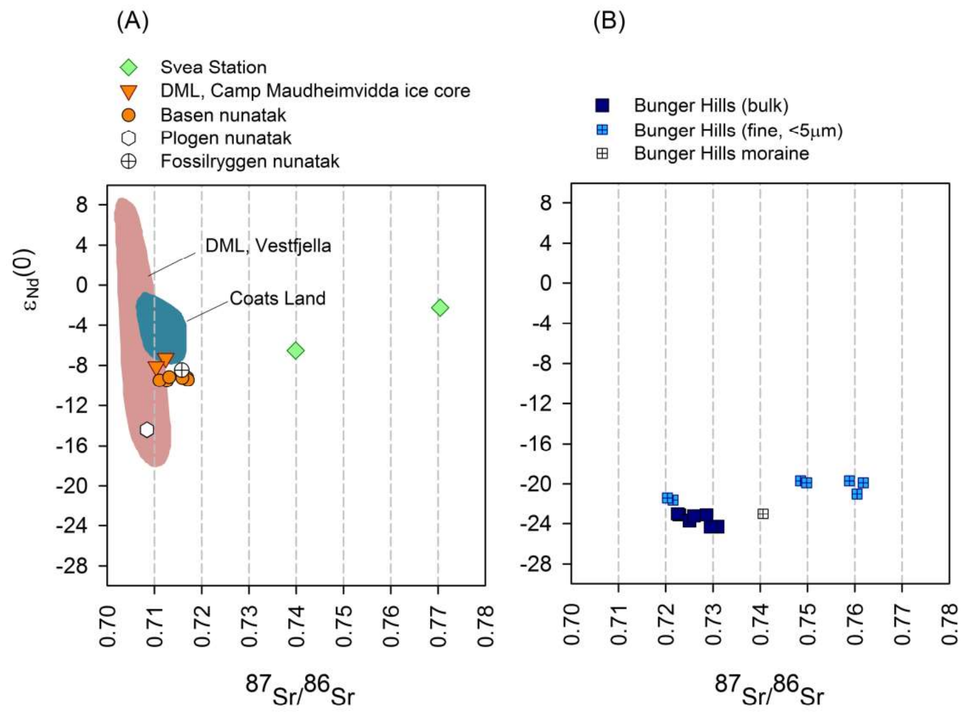

Fig. 7: Sr-Nd isotopic composition of Holocene ice core dust from low elevations sites. (A) Camp Maudheimvidda (CM) ice core in coastal DML, local nunataks (Basen, Ploggen, Fossilryggen) and Svea station. Isotopic fields are drawn from literature data on bulk rocks (basalts, tholeiites, andesites) from the DML area of Vestfjella, and Coats Land dolerites (Luttinen & Furnes, 2000; Harris et al., 1990; Riley et al., 2005; Brewer et al., 1992). (B) Bunger Hills. Sr-Nd isotopic data from bulk (all size included) and fine (<5 µm) dust samples from the Bunger Hills raised beaches in Wilkes Land (see text) as well as one data point from a local moraine (Basile et al. 1997).

253x184mm (300 x 300 DPI)

	Ice core	Coordinates	Age	Dust conc. (ppb) ±St.Dev.	Acc.rate (cm w.eq yr^{-1})	Dust flux (mg m^{-2} yr^{-1})	Altitude (m a.s.l.)	Reference
Ice sections								
Holocene	DOME B	77°05'S, 94°55'E	2.0-11.7 Kyr BP	14.2±8	2	0.28	3650	Delmonte, 2003; This work
	VOSTOK-BH7	78°28'S, 106°48'E	3.6-9.8 Kyr BP	17.8±8	2	0.36	3480	Delmonte et al., 2005
	EPICA-DC	75°06'S, 123°21'E	2.0-11.7 Kyr BP	14.3±8	2.7	0.39	3233	Delmonte et al., 2002
	SOLARICE-DC	123°21' 48''E 75°06'31''S	3.3-4.5 Kyr BP	11.7±5	2.6	0.31	3233	This work
	DOME FUJI	77°19'01"S, 39°42'12"E	3.2-11.7 Kyr BP	20±11	2.7	0.54	3810	Fujii et al., 2003 Kawamura et al., 2017
	EPICA-DML	75°00'S, 00°04'E	2.0-11.7 Kyr BP	25±14	6	1.50	2882	Wegner et al., 2015
	TALDICE	72° 49'S, 159°11'E	2.0-11.7 Kyr BP	25.1±10	7	1.76	2315	Albani et al., 2012 Baccolo et al., 2018
	TAYLOR DOME	77°47'47''S, 158°43'26''E	2.0-11.7 Kyr BP	21±14	6	1.18	2365	Aarons et al., 2016
Firn sections								
Pre-industrial Age	DC ITASE	75°06'S, 123°21'E	1570-1800 AD	8±4	2.5	0.20	3230	Delmonte et al., 2013
	D4 ITASE	75°35'S, 135°49'E	1420-1700 AD	9±4	2.0	0.19	2795	
	MdP-A ITASE	75°32'S, 145°510E	1620-1800 AD	14±3	3.6	0.50	2455	
	TALDICE	72° 49'S, 159°11'E	1420-1810 AD	8±4	8.7	0.75	2315	

Supplementary information

SAMPLES ANALYZED IN THIS STUDY

1- SOLARICE ice core samples

The SOLARICE project is a multi-year Franco-Italian scientific initiative aimed at retrieving and studying Holocene climate and solar variability from a new ice core drilled at Dome C, Concordia Station (East Antarctic Plateau). One of the main goals of SOLARICE is the reconstruction of solar activity across the entire Holocene from high-resolution ^{10}Be analyses and the investigation of the relationship between ^{10}Be and climate/atmospheric circulation changes that are reconstructed through a multiproxy approach including mineral dust aerosol grain size.

The project lead to the recovery of a 204 m deep ice core during the Antarctic summer 2015/16 at about 1.5 km from Concordia station (123° 21,793'E, 75° 06,511'S). In this study, we present preliminary dust grain size data (figure **3B**) obtained from ~5 cm long samples from about 125 to 160 m depth.

2- Camp Maudheimvidda ice core samples

Two ice cores were drilled at Camp Maudheimvidda (CM, 73°06'S, 13°09'W; 360 m a.s.l) in Dronning Maud Land during the Antarctic summer 1997-1998, as part of the EPICA pre-site survey. The cores were drilled 5 m apart and are 100 m deep. Camp Maudheimvidda is situated 140 km from the coast in the Vestfjella mountain range. The site is within tens of kilometers range of several nunataks (Basen, Plogen, Fossilriyggen) and approximately 200 km north of Svea Station. The total time span of the CM core is 300 years (Jonsell et al., 2005).

Two dust samples were extracted from the ice core. Sample DML#1 is the upper 55 m of firn, spanning 30-100 years BP. Sample DML#2 is the lower section, from 55 to 105 m depth, spanning 100-200 years BP. The snow accumulation rate at CM is 220 mm w.eq year^{-1}. (Holmlund et al., 2000). Dust was extracted by filtration and analyzed for Sr and Nd isotopic composition. Samples were collected by Margareta Hansson and Pierre Biscaye.

3- Taylor Glacier moraines

In this work we analyzed the Sr and Nd isotopic composition of the fine fraction (<5 micron) of two sediment samples from Taylor Glacier, Transantarctic Mountains, provided by Dr. Luca Lanci (TG1, TG9). They consist of mixed material from a lateral moraine of the Taylor Glacier where the dominant lithology is Ferrar Dolerite possibly mixed with other lithologies. Results from these two samples (Supplementary Table

S1) have been integrated in Figure 5 inside the "Dry Valleys" group. TG1 coordinates: 161° 45.445'E77°46.152'S; TG9 coordinates: 161° 47.782' E, 77° 43.714'S.

4- Dronning Maud Land nunataks

Nine samples from Basen (73°02'S, 13°24'W), Plogen (73°13'S, 13°50'W) and Fossilriyggen(73°23'S, 13°02'W) nunataks in the Vestfjella mountain range, western DML, were sampled for this study and analyzed for their Sr and Nd isotopic composition. Bedrock in the area is basalt (Sohlenius et al., 2004). Also, two regolith samples were collected close to Svea Station (74°34'S, 11°13'W), located in the Heimefrontsfjella mountain range. There, bedrock consists of metamorphosed red granite and augengneiss (Sohlenius et al., 2004). Samples were collected by Margareta Hansson. The samples were sieved using a 150μm nylon mesh and the fine fraction was used for Sr and Nd analyses.

5- Bunger Hills fossil beach ridges

Seven raised beach deposits from Bunger Hills (Gore et al., 2001), East Antarctica (100°20'E to 101°28'E; 65°58'S to 66°20'S) were analyzed for Sr and Nd isotopic composition (Supplementary Table S1). Both the bulk (all size fractions) and the fine (<5 micron) size fractions were measured. At EUROCOLD (University Milano-Bicocca, UNIMIB), the coarse fraction was removed from bulk samples by using a pre-washed 5 μm SEFAR Nitex® open mesh, while the fraction 0.4μm<∅<5μm was collected on 0.4 μm Isopore™ Polycarbonate membranes. After filtration, the membranes were put into one pre-cleaned Corning tube filled with ~10 mL MQ water, and microparticles were removed from the filter by sonication.

These samples were kindly provided by Dr. P.Augustinus. Organic matter was removed with hydrogen peroxide and carbonates removed with hydrochloric acid. The age of these sediments (Optically Stimulated Luminescence (OSL), Gore et al., 2001) spans from about 21900±3400 years BP to 4800±700 years BP.

METHODS

1- DUST CONCENTRATION AND GRAIN SIZE

About 600 samples were analyzed for concentration and grain size by using in parallel a Beckman Coulter Multisizer 4 and a Beckman Coulter Multisizer 4e, strictly intercalibrated, available in clean rooms ISO6 at EUROCOLD Laboratory, UNIMIB. Analytical protocols are described in Delmonte et al., 2005. Analyses were performed on about 4-5 mL per sample and from the dust volume (mass) size distribution the CPP (Coarse Particle Percentage) parameter was calculated. CPP represents the relative (%) volume or mass fraction included in the size interval between 3-5 µm.

1- STRONTIUM AND NEODYMIUM ISOTOPIC RATIOS

At the Department of Geosciences, Swedish Museum of Natural History (NRM, Sweden) the Taylor Glacier and Bunger Hills samples were evaporated in acid-cleaned 7 mL Savillex beakers. The chemical treatment of the samples including mineral dust digestion and an elemental separation (Rb-Sr and Sm-Nd) using ion exchange chromatography was performed. Here, a line dedicated to the treatment of small dust samples (1-10 ng of Nd and 5-100 ng of Sr in dust for Antarctic ice core samples) was developed (Delmonte et al., 2008). Briefly, the samples were spiked with mixed $^{147}Sm/^{150}Nd$ spike and ^{84}Sr enriched spike for isotope dilution determination of the concentrations. Samples were digested in an acid mixture of 1.5 mL of HNO_3, HF and $HClO_4$ and heated to 90 °C in closed Savillex beakers for three days. The solution was evaporated to complete dryness on a hot plate and the residue re-dissolved in 4 mL 6M HCl. Bunger Hills bulk samples were ground to a powder using a steel mortar and spiked as above. Bulk samples were digested in a mixture of 2 mL HF and 20 drops of HNO_3 in steel bombs in an oven at 205 °C for three days. The solution was evaporated to complete dryness on a hot plate. The residue repeatedly re-dissolved in concentrated HNO_3 (Seastar) and evaporated to remove fluorides. The residue was re-suspended in 5 mL of 6 M HCl and heated in steel bombs at 205 °C for 24 hours. The samples were evaporated and re-suspended in 4 mL 6 M HCl.

To achieve separation of potential interfering elements (Fe, Ba, Rb, Sm, Ce, and Pr), and obtain high column yield and low blanks, the residue was subjected to chemical procedures described in Delmonte et al. (2008). The total blank, including dissolution, chemical separation and mass spectrometry, was frequently monitored in each ion exchange batch and blank concentrations were <4pg for Nd and <80pg for Sr.

Isotopic analysis of Nd and Sr ratios was performed with a Thermo Scientific TRITON Thermal Ionisation Mass Spectrometer (TIMS). Neodymium was loaded mixed with Alfa Aesar colloidal graphite, on double rhenium filaments and analyzed as metal ions in static mode using rotating gain compensation. Concentrations and ratios were calculated assuming exponential fractionation. The calculated ratios were normalized to $^{146}Nd/^{144}Nd$ = 0.7219. Epsilon units are calculated as follows:

$\varepsilon_{Nd}(0) = [(^{143}Nd/^{144}Nd)_{sample}/(^{143}Nd/^{144}Nd)_{CHUR} - 1] \times 10^4$;

CHUR, chondritic uniform reservoir with $(^{143}Nd/^{144}Nd)_{CHUR}$ = 0.512638

The external precision for $^{143}Nd/^{144}Nd$ is estimated from analysis of the nNdß (small samples)and the La Jolla standard.

The resulting precision is ± 0.4 ε –for small samples (<15ng) and ± 0.2 ε for larger samples (>15 ng), as reported in Supplementary Table 2. Accuracy correction was not applied since the mean standard $^{143}Nd/^{144}Nd$ ratios were within error of accepted literature values (nNdß $^{143}Nd/^{144}Nd$ ratio 0.511895 ± 22 (n=20) and LaJolla $^{143}Nd/^{144}Nd$ ratio 0.512863 ± 08 (n=12)).

Total procedural blank levels (blank associated with the digestion in Teflon beakers, ion exchange and instrument) were <25 pg of Nd and are considered negligible.

Strontium samples were spiked with a ^{84}Sr enriched spike and analyzed on a Thermo Scientific TRITON TIMS using a load of purified sample mixed with tantalum activator on a single rhenium filament. Two hundred 8s integrations were recorded in multi-collector static mode, applying rotating gain compensation. Measured ^{87}Sr intensities were corrected for Rb interference assuming $^{87}Rb/^{85}Rb$ = 0.38600 and ratios were calculated using the exponential fractionation law and $^{88}Sr/^{86}Sr$ = 8.375209. The external precision for $^{87}Sr/^{86}Sr$ estimated from analyzing NBS SRM 987 standard was ±16 ppm for large samples (0.710221 ± 11 ; 200 ng loads; n=16) and ± 30 ppm for small samples (0.710222 ± 21 ; 10-50 ng loads n=12). An accuracy correction was applied to the $^{87}Sr/^{86}Sr$ ratios corresponding to a $^{87}Sr/^{86}Sr$ ratio of 0.710245 for NBS SRM 987 standard. Total procedural blank levels were <80 pg of Sr and are considered negligible.

Each preparation batch of Nd and Sr from small dust samples was checked using the basaltic rock, BCR-2, certified reference material. Preparation and analysis of 150 to 600 µg aliquots of BCR-2 gave a concentration precision of ±10% and with literature values highly comparable isotopic results ($^{87}Sr/^{86}Sr$ - 0.705011 ±22).

COMMENT: RESULTS ON FINE AND BULK FRACTIONS OF BUNGER HILLS SAMPLES

Bunger Hills potential source area (PSA) samples were size-segregated to account for Sr fractionation with particle size. With On the whole, the fine Bunger Hills PSA samples have relatively high $^{87}Sr/^{86}Sr$ ratios ($0.720372<^{87}Sr/^{86}Sr<0.761802$ and $-19.7<\varepsilon_{N}d(0)<-21.6$) compared to the bulk samples ($0.722543<^{87}Sr/^{86}Sr<0.730972$ and $-23<\varepsilon_{Nd}(0)<-24.3$; fig. 2). The $^{87}Sr/^{86}Sr$ variations with particle size in the Bunger Hills samples are consistent with previous studies of size-dependent fractionation, finer fractions having a higher Rb/Sr and thus a higher $^{87}Sr/^{86}Sr$ (Andersson et al., 1994; Winton et al., 2016a). The Δ87Sr/86Sr is ~0.028310 units, which is larger than the $^{87}Sr/^{86}Sr$ increase of ~0.0028 units observed between 63 µm and 2 µm of dust particles reported by Gaiero (2007)and 0.00115 units between 63 µm and 10 µm observed by Winton et al. (2016a). Two samples do not fractionate with particle size (BHO95 and BHO98). This could be related to different size fractions originating from different sources. There is also a size effect on the $^{143}Nd/^{144}Nd$ isotopes with an increase of around 3 $\varepsilon_{Nd}(0)$ units for the finer particle size, although this fractionation is less pronounced than that of the $^{87}Sr/^{86}Sr$ fractionation. Most studies found that $^{143}Nd/^{144}Nd$ in dust is independent of particle size. Fine (<5 µm) and bulk Sr and Nd isotope ratios reported in Delmonte et al. (2004); Grousset et al. (1992) also show that $^{87}Sr/^{86}Sr$ are greater in fine particle size while $\varepsilon_{Nd}(0)$ variation with particle size has no clear trend. However, similar to this study, Yokoo et al. (2004) reports Nd isotope ratios in loess were higher in finer grained samples.

REFERENCES for Supplementary Material

Andersson PS, Wasserburg GJ, Ingri J et al. (1994) Strontium, dissolved and particulate loads in fresh and brackish waters: the Baltic Sea and Mississippi Delta. Earth and Planetary Science Letters, 124(1-4), 195-210.

Delmonte B, Basile-Doelsch I, Petit JR et al. (2004). Comparing the Epica and Vostok dust records during the last 220,000 years: stratigraphical correlation and provenance in glacial periods. Earth-Science Reviews, 66(1-2), 63-87.

Delmonte B, Andersson PS, Hansson M et al. (2008). Aeolian dust in East Antarctica (EPICA-Dome C and Vostok): Provenance during glacial ages over the last 800 kyr. Geophysical Research Letters, 35(7).

Gaiero DM (2007) Dust provenance in Antarctic ice during glacial periods: from where in southern South America? Geophysical Research Letters, 34(17).

Gore, D. B., Rhodes, E. J., Augustinus, P. C., Leishman, M. R., Colhoun, E. A., & Rees-Jones, J. (2001). Bunger Hills, East Antarctica: ice free at the last glacial maximum. Geology, 29(12), 1103-1106.

Grousset F, Biscaye P, Revel M et al. (1992) Antarctic (Dome C) ice-core dust at 18 ky BP: Isotopic constraints on origins, Earth and Planetary Science Letters, 111, 175-182.

Holmlund P, Gjerde K, Gundestrup N et al. (2000) Spatial gradients in snow layering and 10 m temperatures at two EPICA-Dronning Maud Land (Antarctica) pre-site-survey drill sites. Annals of Glaciology, 30, 13-19.

Jonsell U, Hansson ME, Mörth CM et al. (2005) Sulfur isotopic signals in two shallow ice cores from Dronning Maud Land, Antarctica. Tellus B: Chemical and Physical Meteorology, 57(4), 341-350.

Sohlenius B, Boström S & Ingemar Jönsson K (2004) Occurrence of nematodes, tardigrades and rotifers on ice-free areas in East Antarctica, Pedobiologia, 48, 395-408, http://dx.doi.org/10.1016/j.pedobi.2004.06.001.

Winton VHL, Dunbar G, Atkins C et al. (2016a) The origin of lithogenic sediment in the south-western Ross Sea and implications for iron fertilization, Antarctic Science, 28, 250-260, 2016a.

Yokoo Y, Nakano T, Nishikawa M et al. (2004) Mineralogical variation of Sr–Nd isotopic and elemental compositions in loess and desert sand from the central Loess Plateau in China as a provenance tracer of wet and dry deposition in the northwestern Pacific. Chemical Geology, 204(1-2), 45-62.

Supplementary Table S1: Bunger Hills samples

SAMPLE CODE	LOCALITY	AGE	
BHO86	Kashalot Island	21900±3400	yr BP
BHO96	Ostronaya Bay	4800±700	yr BP
BHO78	Thomas island	7370±90	^{14}C yr BP
BHO98	Krylatyy inlet	7110±130	^{14}C yr BP
BHO95	Ostronaya bay	6370	^{14}C yr BP
BHO65+66	L.Dolgoe	11000±1200	yr BP
BHO82/83	Thomas island	5780±80	^{14}C yr BP

Sample	type	fraction	[Nd] ppm	[a] ± (ppm)	$^{143}Nd/^{144}Nd$		[b] $2\sigma_{mean}$ *10^6	[c] $\varepsilon_{Nd}(0)$		[d] 2σ	$^{87}Sr/^{86}Sr$		[e] $2\sigma_{mean}$ *10^6	[f] $^{87}Sr/^{86}Sr$ corrected		[g] 2σ*10^6	[Sr] ppm
Camp Maudheimvidda																	
DML#1	ICD	Bulk	18	2	0.512264	±	15	-7.3	±	0.4	0.712386	±	27	0.712386	±	27*	140
DML#2	ICD	Bulk	11	1	0.512222	±	65	-8.1	±	1.3*	0.710378	±	54	0.710378	±	54*	110
DML area																	
Innen Fossilryggen	nunatak	Bulk	7	1	0.512204	±	15	-8.5	±	0.4	0.715777	±	19	0.715777	±	21	46
Basen 1 NO	regolith	<150	37	<1	0.512149	±	01	-9.6	±	0.2	0.712609	±	07	0.712609	±	11	-
Basen 2 NW	regolith	<150	26	<1	0.512151	±	07	-9.5	±	0.2	0.711081	±	09	0.711081	±	11	-
Basen 6 N	regolith	<150	31	<1	0.512168	±	05	-9.2	±	0.2	0.713126	±	12	0.713126	±	12*	-
Basen Aboa 1	regolith	<150	47	<1	0.512165	±	07	-9.2	±	0.2	0.716941	±	15	0.716941	±	15*	-
Basen Aboa 2	regolith	<150	47	<1	0.512154	±	07	-9.4	±	0.2	0.717059	±	27	0.717059	±	27*	-
Basen Aboa 2 *duplicate*											*0.716970*	±	*10*	*0.716970*	±	11	-
Basen Aboa 3	regolith	<150	43	<1	0.512164	±	09	-9.2	±	0.2	0.715899	±	09	0.715899	±	11	-
Plogen toppen 1	regolith	<150	15	<1	0.511899	±	07	-14.4	±	0.2	0.708413	±	09	0.708436	±	11	-
Plogen toppen 2	regolith	<150	18	<1	0.511900	±	06	-14.4	±	0.2	0.708423	±	10	0.708446	±	11	-
Svea 1	station	<150	140	<1	0.512304	±	08	-6.5	±	0.2	0.739869	±	11	0.739869	±	11	-
Svea 2	station	<150	57	<1	0.512524	±	04	-2.2	±	0.2	0.770459	±	09	0.770459	±	11	-
Taylor Glacier																	
TG 1	moraine	<5	20	2	0.512134	±	15	-9.8	±	0.4	0.718521	±	08	0.718544	±	21	160
TG 9	moraine	<5	10	1	0.512350	±	290	-6.0	±	5.7*	0.712139	±	12	0.712162	±	21	940
Bunger Hills																	
BHO 83	Fossil beach ridge	Bulk	21	<1	0.511390	±	07	-24.3	±	0.2	0.730949	±	05	0.730972	±	11	860
BHO 83	Fossil beach	<5	30	3	0.511628	±	23	-19.7	±	0.5*	0.748501	±	07	0.748524	±	21	120

	ridge																
BHO 96	Fossil beach ridge	Bulk	20	<1	0.511453	±	07	-23.1	±	0.2	0.722871	±	05	0.722894	±	11	360
BHO 96	Fossil beach ridge	<5	60	6	0.511560	±	10	-21.0	±	0.4	0.760460	±	23	0.760483	±	23*	170
BHO 78	Fossil beach ridge	Bulk	62	<1	0.511393	±	02	-24.3	±	0.2	0.729460	±	04	0.729483	±	11	280
BHO 78	Fossil beach ridge	<5	50	5	0.511626	±	19	-19.7	±	0.4	0.758841	±	09	0.758864	±	21	130
BHO 98	Fossil beach ridge	Bulk	37	<1	0.511461	±	04	-23.0	±	0.2	0.722520	±	06	0.722543	±	11	340
BHO 98	Fossil beach ridge	<5	50	5	0.511530	±	07	-21.6	±	0.2	0.721545	±	06	0.721568	±	21	380
BHO 95	Fossil beach ridge	Bulk	22	<1	0.511424	±	06	-23.7	±	0.2	0.725008	±	05	0.725031	±	11	320
BHO 95	Fossil beach ridge	<5	60	6	0.511542	±	22	-21.4	±	0.4	0.720349	±	05	0.720372	±	21	520
BHO 65+66	Fossil beach ridge	Bulk	29	<1	0.511450	±	04	-23.2	±	0.2	0.725945	±	04	0.725968	±	11	310
BHO 65+66	Fossil beach ridge	<5	80	8	0.511617	±	09	-19.9	±	0.2	0.761779	±	13	0.761802	±	21	160
BHO 86	Fossil beach ridge	Bulk	38	<1	0.511455	±	04	-23.1	±	0.2	0.728599	±	05	0.728622	±	11	280
BHO 86	Fossil beach ridge	<5	100	10	0.511616	±	06	-19.9	±	0.2	0.749795	±	08	0.749818	±	21	240

Supplementary Table S2: Nd and Sr concentrations[in parentheses] and isotopic composition of ice core/snow samples and potential source area samples analyzed in this study.

ICD= Ice Core Dust sample
[a)]Error due to difficulty of measuring small sample masses, estimated by repeat weighting BCR-2 standards (~0.3 mg).
[b)]Internal precision, 2 standard errors of the mean.
[c)]Nd isotopic ratios expressed as epsilon units $\varepsilon_{Nd}(0) = [(^{143}Nd/^{144}Nd)sample/(^{143}Nd/1^{44}Nd)CHUR-1]x10^4$;
CHUR, chondritic uniform reservoir with $^{143}Nd/^{144}Nd$=0.512638.
[d)]Uncertainty estimates based upon external precision for standard runs. Internal precision is used if it exceeds the external.
[e)]Internal precision, 2 standard errors of the mean.
[f)]An accuracy correction was applied to Taylor Glacier and Bunger Hills samples,
while the $^{87}Sr/^{86}Sr$ ratio for the NBS 987 standard was 0.710222 ±22 (n=12). Corrected to a NSB 987 $^{87}Sr/^{86}Sr$ ratio of 0.710245.
[g)]Uncertainty estimates based upon external precision for standard runs. * Internal precision is used if it exceeds the external.